A global three-dimensional model study of carbonaceous aerosols

C. Liousse, J. Penner, C. Chuang, J. Walton, H. Eddleman, H. Cachier

JOURNAL OF GEOPHYSICAL RESEARCH, VOL. 101, NO. D14, PAGES 19,411-19,432, AUGUST 27, 1996

A global three-dimensional model study of carbonaceous aerosols

C. Liousse,[1] J.E. Penner,[2] C. Chuang, J.J. Walton, and H. Eddleman
Global Climate Research Division, Lawrence Livermore National Laboratory, Livermore, California

H. Cachier
Centre des Faibles Radioactivités, Centre National de la Recherche Scientifique-Commissaerat à l' Energie Atomique, Gifsur Yvette, France

Abstract. We have developed detailed emission inventories for the amount of both black and organic carbon particles from biomass burning sources (wood fuel, charcoal burning, dung, charcoal production, agricultural, savanna and forest fires). We have also estimated an inventory for organic carbon particles from fossil fuel burning and urban activities from an existing inventory for fossil fuel sources of black carbon. We also provide an estimate for the natural source of organic matter. These emissions have been used together with our global aerosol model to study the global distribution of carbonaceous aerosols. The accuracy of the inventories and the model formulation has been tested by comparing the model simulations of carbonaceous aerosols in the atmosphere and in precipitation with observations reported in the literature. For most locations and seasons, the predicted concentrations are in reasonable agreement with the observations, although the model underpredicts black carbon concentrations in polar regions. The predicted concentrations in remote areas are extremely sensitive to both the rate of removal by wet deposition and the height of injection of the aerosols. Finally, a global map of the aerosol single scattering albedo was developed from the simulated carbonaceous particle distribution and a previously developed model for aerosol sulfates. The computed aerosol single scattering albedos compare well with observations, suggesting that most of the important aerosol species have been included in the model. For most locations and seasons, the single scattering albedo is larger than 0.85, indicating that these aerosols, in general, lead to a net cooling.

1. Introduction

It is important to quantify the climate forcing by anthropogenic aerosols in order to understand the cooling effect they might have had on the climate system relative to the warming by anthropogenic greenhouse gases. *Charlson et al.* [1991] and *Penner et al.* [1992] have shown that due to their tropospheric geographical distribution, their size and their optical properties, sulfates and carbon particles may have a net cooling effect which could be as important as the heating effect by anthropogenic greenhouse gases. Several studies have focused on the role of the sulfates, modeling the transport of these aerosols at different scales [*Langner and Rodhe*, 1991; *Luecken et al.*, 1991; *Penner et al.*, 1994; *Pham et al.*, 1995; *Anderson and Boucher*, 1994; *Benkovitz et al.*, 1994], and the forcing by anthropogenic sulfate aerosols has been estimated [*Charlson et al.*, 1991; *Kiehl and Briegleb*, 1993] as well as their climate effect [*Taylor and Penner*, 1994; *Penner et al.*, 1996]. In contrast, very few modeling studies of the importance of black carbon particles currently exist [*Penner et al.*, 1991a; *Penner et al.*, 1992; *Cooke and Wilson*, this issue] and there are no previous global model studies of organic carbon particles.

Carbonaceous particles consist of highly polymerized organic material with a low content of hydrogen and oxygen. This aerosol is usually divided in two fractions, black carbon (BC) and organic carbon (OC). Black carbon particles are defined on the basis of their strong absorption of solar radiation and their refractive behavior to thermal and chemical attacks [*Wolff and Klimish*, 1982; *Novakov*, 1982]. This resistance, together with the fact that the most important source of BC is combustion, means that BC is able to act as an important tracer of industrial pollution. Observations in both remote and source areas indicate that the OC fraction of the carbonaceous aerosol is always larger than the BC fraction [*Cachier*, 1995]. In contrast to BC, these particles have a refractive index that is close to that of the sulfates and therefore mainly scatter solar radiation.

Very near sources of primary aerosol and in areas of new particle formation, carbonaceous particles may be mainly externally mixed. However, in most places in the atmosphere, carbonaceous particles appear to be present as a heterogeneous mixture of carbon, sulfates, and other components [*Langner et al.*, 1992; *Parungo et al.*, 1994; *Liousse et al.*, 1993], a property which results from their ability to adsorb and condense gases with low vapor pressures. This gives them a hydrophilic behavior, allowing them to act as cloud condensation nuclei. They should therefore have an indirect radiative impact through their effects on cloud albedo [*Penner et al.*, 1992; *Novakov and*

[1]Now at Centre des Faibles Radioactivités, Centre National de la Recherche Scientifique-Commissareat à l' Energie Atomique, Gif sur Yvette, France.

[2]Now at Department of Atmospheric, Oceanic, and Space Sciences, University of Michigan.

Paper number 95JD03426.
0148-0227/96/95JD-03426$09.00

Penner, 1993]. In addition, consideration of the condensation of sulfate vapor onto carbonaceous aerosols implies that the estimation of the global direct radiative effect of sulfate particles cannot be obtained from a simple addition of the forcing by carbonaceous particles and the forcing by anthropogenic sulfate particles because the size distribution of the sulfate formed by gas to particle conversion (and hence its specific scattering coefficient) will depend on the size distribution of carbonaceous aerosol [*Chuang and Penner*, 1995]. Hence it is important to model both the sulfate and carbonaceous aerosol systems in order to correctly estimate anthropogenic forcing.

Experimental data [*Cachier*, 1992] indicate that carbonaceous particles are mainly emitted by combustion sources and that most of these are of anthropogenic origin (compare *Penner* [1995]). Sources from fossil fuel combustion occur mainly in the northern hemisphere north of 20N, whereas sources from biomass burning are primarily distributed in tropical areas. We note that the sources from biomass burning are poorly known, especially those ascribed to domestic and agricultural fires [*Cachier,* 1992]. In addition, the areas associated with savanna and forest burning are uncertain to a factor of 2 [*Lacaux et al.,* 1995]. Natural fires of the temperate and boreal areas are also poorly quantified but are small on a global basis. They were not included in our inventory.

The natural emissions of carbonaceous particles result from two sources: photochemical conversion of the gaseous emissions from vegetation to species with low vapor pressures and direct emission of particles from plants. Both sources need better quantification. Modeling studies have shown that roughly 0.1 to 8% of terpenes oxidize to species which may condense, while the oxidation of isoprene is much less efficient at producing particles under ambient conditions [*Pandis et al.*, 1991]. We include the terpene source here but ignore the direct emission of particles from vegetation as well as the production and transport of microorganisms. Both of these latter sources are thought to be mainly in size ranges above 1-μm diameter.

Carbonaceous particles have a short residence time (range of 3-7 days); hence hemispheric particle exchange is negligible. The short residence time, coupled with the multiplicity of sources described above, leads to concentrations ranging from ~1 $\mu g\ m^{-3}$ in rural source areas to <1 $ng\ m^{-3}$ in remote regions such as the south pole. The removal of these particles from the atmosphere occurs by both dry and wet deposition. As shown by *Ducret and Cachier* [1992], the latter process is by far the most important.

The focus of this study is a model calculation of the global distribution of carbonaceous particles. For this purpose, we use the global three-dimensional (3-D) transport model, Grantour [*Walton et al.*, 1988; *Penner et al.,* 1991b].

Below, we first describe the emission inventory of the carbonaceous particles that we use in the model. A detailed inventory for the biomass burning sources is developed. A description of the fossil fuel sources is presented. A tentative estimate for the natural source contribution is presented. Then we present the results for a global distribution of carbonaceous particles obtained from these inventories and the Grantour model. The sensitivity of model results to a variety of parameterized processes is examined. Then a detailed comparison between observations and model predictions of the spatial, temporal, and vertical distribution of carbonaceous particles is presented. Finally, the global distribution of aerosol single scattering albedos obtained from BC, OC, and sulfate concentrations is reported and compared to available observations.

2. Emission Inventory of Carbonaceous Particles

2.1. Biomass Burning Sources

Here, we develop a global emission inventory of biomass burning particles. Unlike previous inventories, we take into account savanna, forest, agricultural, and domestic fire sources of particles. Savanna and forest fires for tropical Africa, tropical America, tropical Asia and Australia are taken from the work of *Hao et al.* [1990] and *Dignon and Penner* [1991] but are updated as noted below. Because of the lack of data (especially for agricultural and domestic fires), a number of assumptions had to be made. Thus this inventory represents our best initial estimate but may be revised in the future. Because of their separate radiative characteristics, separate emission factors have been developed for BC aerosol and the total particle (TP) emission factor. Emission factors represent the fraction of total emissions with diameter <1 μm. Indeed, whereas concentration data are usually provided by instruments with a cutoff of 2.5 μm, a number of size-resolved observations indicate that most of the carbonaceous particle mass has a diameter of less than 1 μm. The particles produced by biomass burning are a complex mixture of BC, OC, and other constituents. In addition, OC represents only a fraction of the total organic matter present in the aerosol because OC is a measure of carbon mass, whereas the total organic matter is a measure of the total mass chemically bound to carbon and therefore includes, in addition to carbon, hydrogen atoms, oxygen atoms, and minor amounts of other species. Also, smoke aerosols (TP) include a number of other components (nitrates, sulfates, etc.). In our comparison to data, for example, we assumed that the calculated global mean fraction of the TP-BC that is organic matter (OM) was 85%. Also, for comparison to measurements, we have assumed that OM/OC = 1.3.

Savanna and forest fires. Savanna and forest fires are the most important particle sources from biomass burning [*Levine*, 1990]. The transport, removal, and distribution of particles from these sources were studied previously [*Penner et al.*, 1991a]. Here, we reevaluate the emissions from these sources, taking into account recent analysis of emission factors and of the total amount of fuel burned.

Penner et al. [1991a] used inventories of the total amount of fuel burned developed by *Hao et al.* [1990] for tropical Africa, tropical America, and tropical Asia, while those for Australia were from J. Dignon (personal communication, 1990). However, African savannas are constituted by a mixture of tall and short grass plants instead of tall grass only, as had been assumed by *Hao et al.* [1990]. Consequently, we assumed that the savanna plant density was 5 ton/ha rather than 6.6 ton/ha, as assumed by *Hao et al.* [1990] [see *Delmas et al.,* 1991; *Menaut et al.,* 1991]. Additionally, the frequency of burning is smaller than that assumed by *Hao et al.* [1990]. Hence we assume that 55% instead of 75% of African savannas are burned each year [*Menaut et al.*, 1991]. Furthermore, we decreased the mean combustion efficiency (here defined as the fraction of biomass submitted to fires that actually burns) of the savannas from 83 to 80% [*Menaut et al.*, 1991; *Lacaux et al.*, 1995].

The forest fire inventory of burnt biomass followed the inventory of *Hao et al.* [1990]. Further work would be needed to include recent results on the density of the burnt aboveground biomass of forest trees. *Brown et al.* [1989] show that the standing biomass could be 27% higher than that of *Hao et al.* [1990; *Hao and Liu,* 1994]. Also, further work would be

Table 1. Inventory of the Yearly Emissions of Black Carbon Particles and Organic Matter

Products, Tg/yr	Organic Matter, Tg of mass/yr	Black Carbon, Tg C/yr
Biomass burning	44.6	5.63
Savannas	15.5	2.17
Tropical forests	16.6	1.93
Agricultural fires*	3.1	0.53
Domestic fuels†	9.3	1.
Fossil fuel	28.5	6.64
Natural sources	7.8	-----
Total	81	12.3

* Agricultural fires: included are wheat, barley, rye, corn, rice, and sugar cane.
†Domestic fuels: fuel wood, bagasse, charcoal, and dung.

necessary in order to improve the estimates of the amount of burning in South America that we took into account (R. Chatfield, personal communication, 1995).

We also updated the BC and TP emission factors used by *Penner et al.* [1991a]. The nature of the burning condition affects the combustion efficiency, the particulate production rate, and the fraction of particulate that is BC. Indeed, the TP emission factor of savanna fires is less than half that of forest fires: we chose a mean value of 8.1 ± 5.5 g TP per kg of fuel for savanna fires and 18 ± 10 for forest fires. The ratio of BC to TP (BC/TP) emissions is ~10% for savanna fires and ~8.5% for forest fires. These mean emission factors and BC/TP values for savanna fires were estimated from both ground [*Liousse et al.*, 1995; *Cachier et al.*, 1995] and aircraft [*Andreae et al.*, 1993; *Le Canut et al.*, 1996] measurements, whereas those for forest fires are from aircraft measurements only [*Radke et al.*, 1988; *Ward et al.*, 1991].

The total source of organic matter from savanna and forest fires is ~32 Tg/yr (see Table 1), considerably lower than would be obtained from previous estimates of the source of particles from savanna and forest burning [*Penner et al.*, 1992]. Annual BC emissions are higher for savanna fires (2.2 Tg/yr) than for forests fires (1.9 Tg/yr), but the annual OM emissions (assumed to be 85% of the TP-BC emissions) are higher for forest fires (17 Tg/yr) than for savanna fires (~16 Tg/yr).

Figure 1 shows the mean temporal distribution of the savanna and forest fires in the northern and southern hemispheres as developed by *Hao et al.* [1990]. This distribution has been shown to agree with experimental data and satellite observations registered in the last 10 years [*Riehl*, 1979; *Delmas et al.*, 1991; *Menaut et al.*, 1991] although differences can occur in any given year due to shifts in rainfall timing and amounts. The long-term pattern of BC measurements observed in source regions in Brazil [*Artaxo et al.*, 1994] and the Ivory Coast [*Liousse et al.*, 1994] has also confirmed our choice of the temporal distribution.

Domestic fires. Domestic fires are an important source of both BC and TC particles. Indeed, this source has been regularly increasing in the tropics and is predicted to increase in the future as a result of increasing population. As an example, the use of firewood in India is predicted to increase by a factor of 3 between 1985 and 2015 [*Hammond*, 1992]. We divided the domestic fires into two parts: those due to fuel wood consumption and those due to agricultural fires. Indeed, due to the scarcity of trees in some countries, substitutes have been found in agricultural wastes or, for the poorest countries, in animal wastes or dung. For example, 2/3 of the rural energy in China comes from agricultural fires [*Crutzen and Andreae*, 1990]. In India, 50% of the burnt biomass amounts are due to wood burning, whereas dung and agricultural waste burning constitute the other half.

While wood fuels have been considered in the past, a global inventory that takes into account all of the fuels used in domestic fires has never been developed. It is important to note that many assumptions are required to develop such an inventory. An exhaustive literature survey was conducted to develop this inventory.

As noted by *Seiler and Crutzen* [1980] and *Strehler and Stutzle* [1987], nearly 81% of the total wood harvest is used for domestic purposes in the developing countries, whereas only 19% is used in this manner in the developed countries. In the following, we used the definitions of developing and developed countries given by the Food and Agriculture Organization (FAO) [1991]. For example, the whole of Africa, including South Africa, was assumed to be developing, in spite of the fact that much of South Africa may be classified as developed. Also, in the developing countries, the northern and the southern hemispheres were differentiated because the occurrence of some domestic fires is governed by the establishment of the dry or wet season, which depends on the specific locale considered.

Fuel wood sources. The global distribution of fuel wood, bagasse (a fuel material derived from sugar cane wastes), and charcoal consumption was obtained from the FAO data on production, importation, exportation, stock changes and losses [*FAO*, 1991]. Within each country the burning of these fuels was distributed by population.

The burnt biomass amounts of the developed countries were calculated from this distribution, assuming a combustion efficiency of 90% [*Seiler and Crutzen*, 1980; *Robinson*, 1989]. Particulate emissions from wood vary between 5 and 20 g/kg fuel, a variability which is mainly linked to the nature of the wood and its water content [*Butcher and Sorenson*, 1979; *Cooper*, 1980; *De Angelis et al.*, 1980; *Butcher and Ellenbecker*, 1982; *Dasch*, 1982; *Muhlbaier and Williams*, 1982; *Piispanen et*

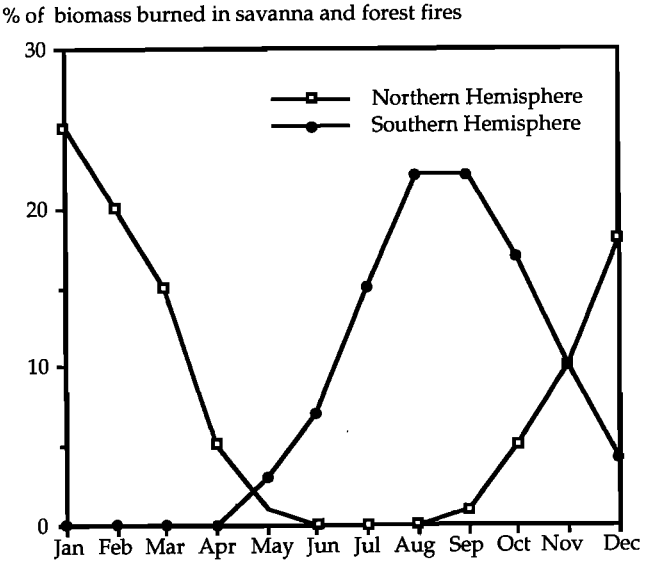

Figure 1. Temporal distribution of savanna and forest fires in the northern and southern hemispheres (given each month in percent of total biomass burned).

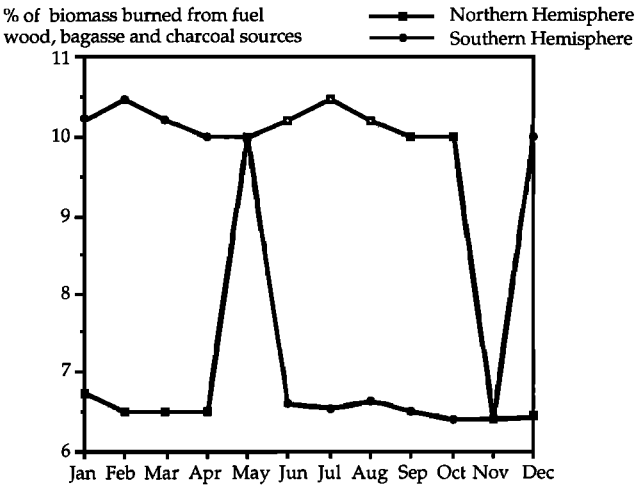

Figure 2. Temporal distribution of fuel wood, bagasse and charcoal sources in developing countries for the northern and southern hemispheres (given each month in percent of total biomass burned).

al., 1984; *Sexton et al.*, 1984; *Penner et al.*, 1993; *Turn et al.*, 1993]. For example, the emission factor (EF) for TP for coniferous wood and synthetic wood is 15 g/kg fuel, that of deciduous wood, 7. Also, the dryer the wood, the lower the particulate emission factor. Taking into account all of these conditions, we chose 11 g/kg fuel as the emission factor for the fuel wood sources. A BC/TP ratio of 12% was estimated from the same references.

In the developing countries, nearly 50% of the fuel wood was assumed to be burnt for heating and cooking and 50% for charcoal making [*Openshaw*, 1974; *Delmas et al.*, 1991]. Indeed, the ease in moving and storage of charcoal makes its use as a fuel for villages and cities more desirable than that of wood. Thus we have considered three fuel sources of biomass burning particles: the burning of fuel wood for domestic purposes and for charcoal making, and charcoal consumption. Following *Seiler and Crutzen* [1980] and *Hao et al.* [1990], a combustion efficiency of 90% was assumed for the burnt biomass amounts from the use of fuel wood. A lower value (~20%) was assumed for charcoal making because the wood is incompletely burned during this production [*Strehler and Stutzle*, 1987; *Andreae*, 1991; *Héry*, 1993]. The particulate emission factors and the BC/TP percentages are of the order of 10 g/kg fuel and 15% for charcoal consumption and 17 g/kg fuel and 5% for charcoal making [*Smith et al.*, 1983; *Butcher et al.*, 1984; *Turn et al.*, 1993]. Further investigation is needed to improve these estimates of emission factors.

In the developed countries, we assumed that the particulate emissions from fuel wood, bagasse, and charcoal take place only during the winter season, with the same relative weighting for the months from October through March. In the developing countries, the temporal distribution of these sources is presented in Figure 2. The monthly distribution of each source type was specified according to each of their uses. For example, of the 50% of fuel wood used for direct domestic purposes, 70% is used for cooking, which occurs throughout the year, and 30% is used for heating, whose usage is concentrated in the winter months or during the wet season. The remaining 50% of fuel wood fires are used for charcoal making, a process which occurs outdoors according to *Héry* [1993] and was therefore assumed to take place during the dry season. Likewise, 70% of charcoal consumption is for cooking and was assumed to occur with the same intensity each month, whereas 30% is used for heating and was assumed to occur during the wet season.

Plate 1a summarizes the global distribution of BC emissions from fuel wood, charcoal, and bagasse as obtained from the calculations described above together with those from dung (whose derivation we describe below). As shown, BC emissions take place throughout the world, partially explaining the worldwide presence of this aerosol type.

Agricultural fires. The global distribution of crop production was taken from data compiled by the *FAO* [1991]. The production of wheat, barley, rye and other grains, corn, rice, and sugar cane were considered in our inventory. The following relationships were used to convert maps of production into maps of particulate emissions:

$$(TP) = (M) \times EF(TP)$$

$$(M) = (P) \times (W/P) \times (Wf/W) \times (ce)$$

where TP is the emissions of particles, EF(TP) is the TP emission factor, M is the amount of burnt biomass, Wf is the amount of agricultural waste submitted to fires, W is the total amount of agricultural waste, P is the mass of grains, and ce is the combustion efficiency.

The ratio W/P may be estimated from the harvest index of each crop as given by *Irvine* [1983], *Fisher and Palmer* [1983], *Fischer* [1983], *Barnard and Kristoferson* [1985], and *Strehler and Stutzle* [1987]. For example, total agricultural waste is nearly 1.2 times the amount of grains produced. We followed *Fisher and Palmer* [1983] in estimating the wastes of corn. For the developed countries, corn waste was 1 times its production, while it was 1.85 times its production in the developing countries.

The fraction of agricultural wastes submitted to fires is highly uncertain because it is a random process that has never been quantified. In the developed countries, according to J. Amthor (personal communication, 1995) and in agreement with *Hao et al.* [1990], only 2 to 10% of agricultural wastes are burned. We assumed a fraction of 5% for most of the grains and 10% for rice, but we note that this range is considerably lower than that assumed by *Middleton and Darley* [1973], which ranged from 37 to 50%. In the developing countries, except for rice, we assumed that 30% of the wastes were burned, in agreement with *Robertson and Rosswall* [1986], *Andreae* [1991], and *Hao et al.* [1990]. In the case of rice, we assumed that 50% of the wastes were submitted to fires. Indeed, at least 33% of rice waste is used as fuel in Bangladesh [*Mahtab and Islam*, 1984] and 1-33% in Africa according to *Hao et al.* [1990]. According to *Barnard and Kristoferson* [1985] and K. Cassman (personal communication, 1995) 55 to 60% is burnt on a global basis. In addition, according to *Irvine* [1983] and *Strehler and Stutzle* [1987], 52% of the by-products of the sugar cane are made into bagasse and would be used as a fuel for the sugar industry, whereas nearly 34% would be burnt as open fires. Let us note that in Hawaii, the remaining 14% constituted by underground and aboveground sugar cane biomass is also burnt for electricity supply. In our inventory, we considered the fiber by-products of the sugar cane which are used as a fuel and not registered in the bagasse inventory previously discussed. We also included the open fires of sugar cane waste left in the field.

In the developed countries, agricultural fires are used mainly to clear the fields or in preparing for the next crops. Thus these have been assumed to occur as an open process. In the developing countries, only 40% of agricultural waste fires take

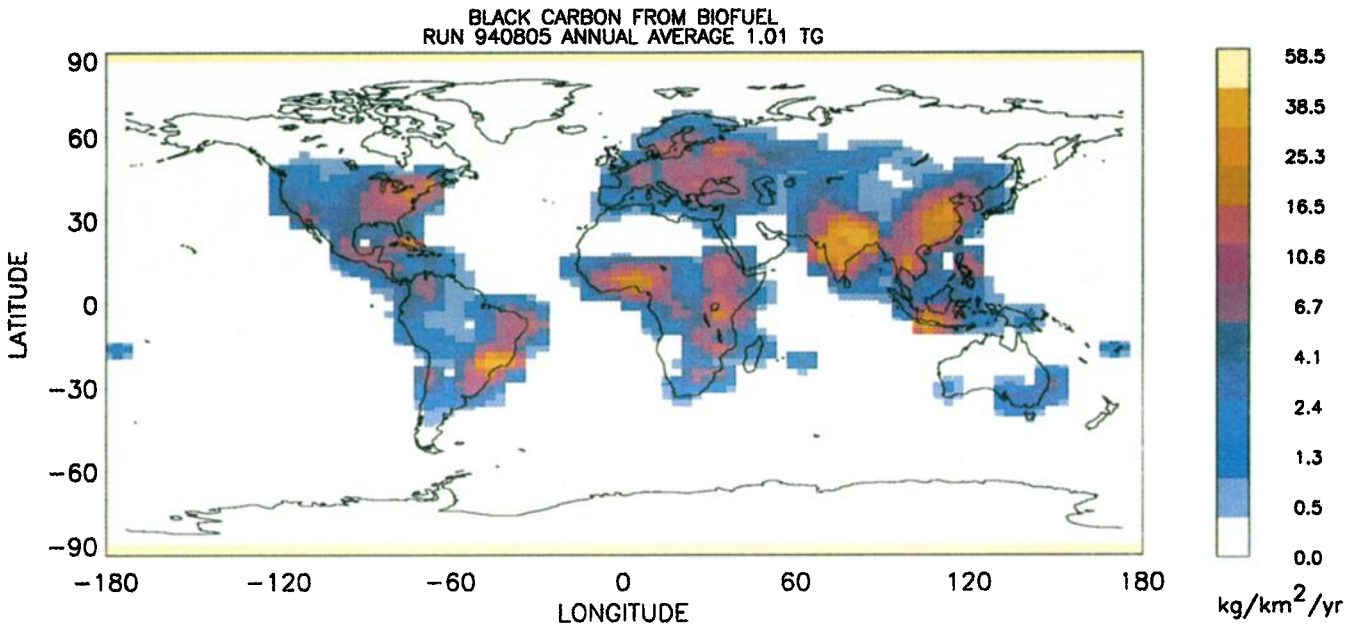

Plate 1a. Distribution of domestic fuel sources of black carbon particles from biomass burning in kgC/km^2/yr.

place as open fires, while 60% of the agricultural by-products submitted to fires is devoted to use as a domestic fuel. The fractions used for domestic and open burning are important because the combustion efficiency as well as the temporal distribution of emissions is impacted. As shown in Table 2, rice burning used as a fuel in domestic fires usually occurs under smoldering conditions. As a result, this burning has a higher particulate emission factor with a relatively low BC fraction compared to the emission factors of open fires. Values of emission factors, BC/TP ratios, and combustion efficiency were estimated from the work of *Meland and Boubel* [1966], *Gerstle and Kemnitz* [1967], *Carroll et al.* [1977], *Darley et al.* [1966], *Seiler and Crutzen* [1980], *Crutzen and Andreae* [1990], *Jenkins et al.* [1991, 1993], and *Turn et al.* [1993]. The different emission factors for smoldering and open-fire emissions have been taken into account for each group of agricultural fires. Table 3 presents a summary of the fraction of waste burned, net emission factor, and net BC to TP ratio for the agricultural emissions included in our inventory. As we may note, the by-products constituted by stalks and fiber such as maize and sugar cane are seen to have a lower combustion efficiency (ce) than that of other wastes [*Robinson,* 1989]. The combustion efficiency of rice burning is higher than that of other grains, as its burning occurs at around 550 K and is therefore more complete. Also, the particulate emission factor is lower than for the other grains, and the ratio of emissions of BC to TP is higher by a factor of 2. It is important to

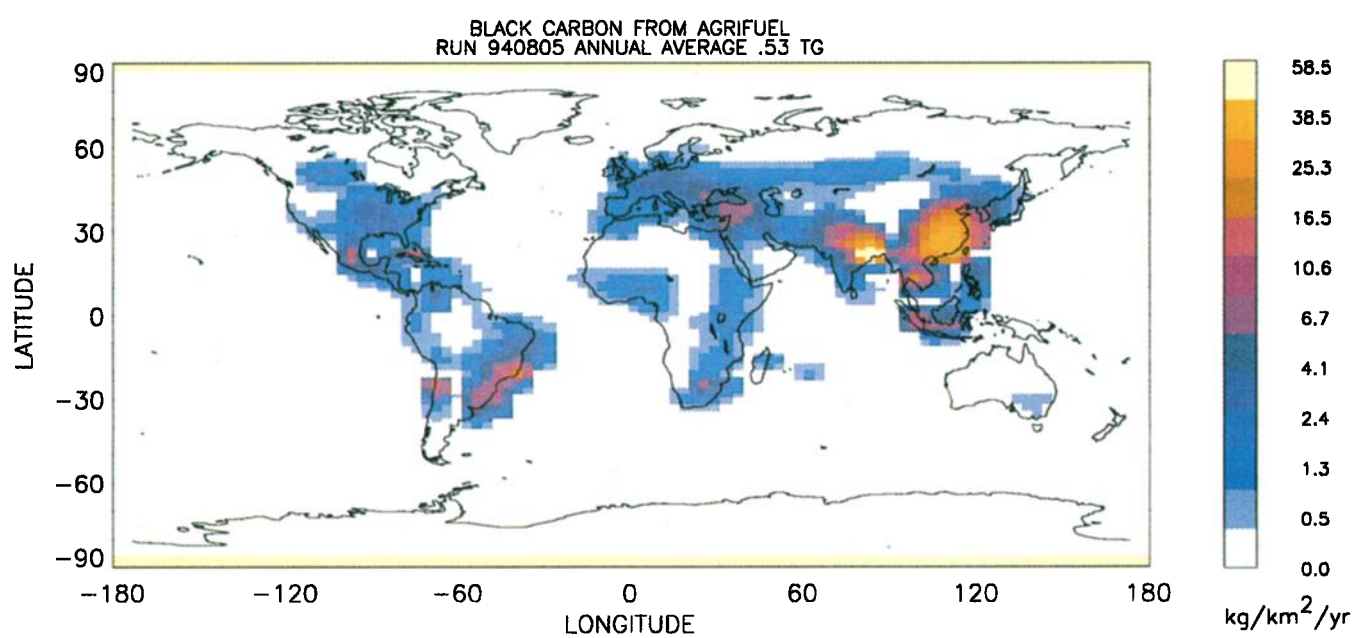

Plate 1b. Distribution of agricultural fire sources of black carbon particles in kgC/km^2/yr .

Table 2. Description of the Parameters Needed to Convert the Production of Rice Grain Into Particulate Emissions From Rice Straw Burning

Rice	Developed Countries (Open fires)	Developing Countries (Mix of Open Fires and Fuel Use)
Agricultural waste per unit of grain	1.2	1.2
Percent of agricultural waste burned	10	50
Combustion efficiency, %	85	85
Nature of fires	Flaming	Smoldering
EF(TP), %	0.25	0.53
Temporal distribution	Harvest	Yearly

note that such parameters are also linked to the moisture content of the by-products before the fire. According to *Carroll et al.* [1977], *Jenkins et al.* [1991], and *Turn et al.* [1993], the emission factor for rice burning was chosen for a moisture content of 10%.

As we noted above for fuel wood, the temporal distribution of emissions from agricultural fires needs to account for the different uses of agricultural fires. An example is shown in Table 2. Agricultural open fires were assumed to appear during the harvest period. For example, from the results of K. Cassman and J. Amthor (personal communications, 1995) and following *Barnard and Kristoferson* [1985], two seasons of harvest (April-May and September-November) have been selected for rice burning in the developed countries. However, this choice ignores the fact that in some countries, instead of two crops devoted to the rice production, one is kept for wheat production. Figures 3a and 3b summarize our assumptions concerning the mean temporal distribution of the total mass burned each month in the developed and the developing countries, respectively. Plate 1b presents the annual average distribution of BC sources from agricultural burning (including all the grains and sugar cane except the bagasse sources) that we obtained from our inventory. The figure shows the importance of these sources in the developing countries of South America and Asia.

Dung sources. As noted above, in some developing countries where fuel wood and grains are scarce, animal wastes are used as a fuel. Inventories were difficult to establish, and our study was based on *Barnard and Kristoferson's* [1985] results. The number of animals whose dung was known to be used as fuel were

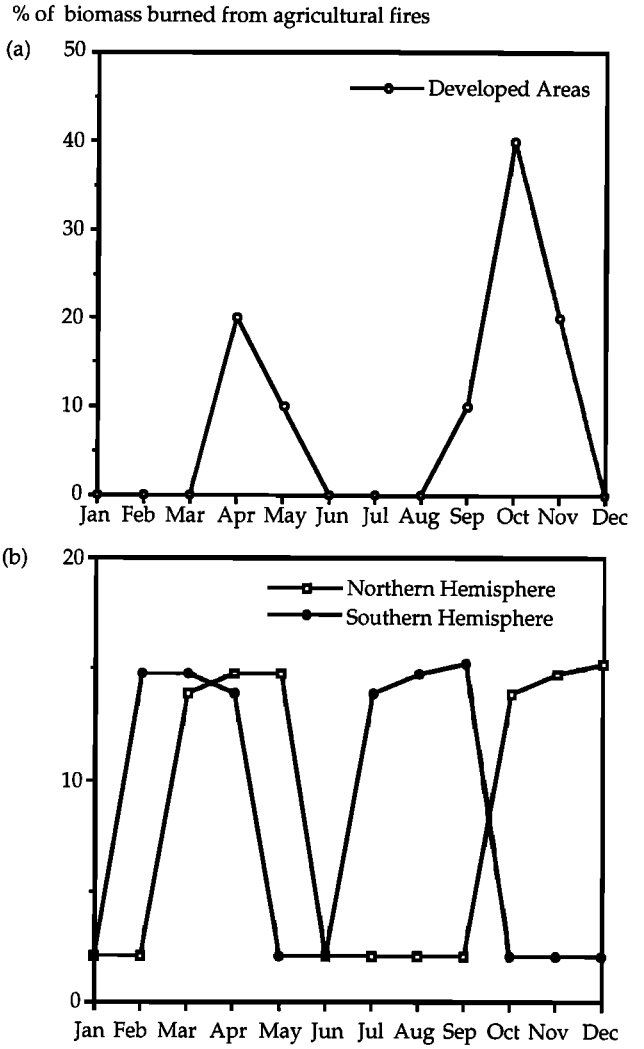

Figure 3. Temporal distribution of agricultural fires in the (a) developed and (b) developing countries (given each month in percent of total biomass burned).

spatially distributed. These data have been converted into dung production by assuming that 0.15 to 1.5 tons of dung are produced per animal per year. Nearly 18.5% of this production is assumed to be submitted to fires. According to recent experiments on African elephant pellets (H. Cachier, personal communication, 1995), we assumed this incomplete burning may be characterized by a combustion efficiency of 50% with a total particulate emission factor of 20 g C/kg of dry matter (kgdm). The BC/TP ratio was taken as 5%. Since the main use of dung burning is linked to cooking, the temporal distribution of this source was evenly distributed throughout the year.

The total amount of BC particles and OM emitted by domestic and agricultural fires is 1.53 Tg/yr and 12.4 Tg/yr, respectively. Table 1 shows that this source represents of the order of 25% of the total biomass burning inventory. Roughly 70% of this total is due to fuel wood, bagasse, dung, and charcoal burning, and 30% to agricultural fires.

Table 3. Combustion Efficiency and Particulate Emission Factors for Different Agricultural Fires

	ce, %	EF(TP), %	BC/TP, %
Rice			
Developed countries	85	0.25	24
Developing countries	85	0.53	16.3
Wheat, rye, and other grains			
Developed countries	70	0.7	13
Developing countries	70	1.2	10
Corn and sugar cane			
Developed countries	35	0.5	14
Developing countries	35	1.2	8
Sugar cane			
Developed countries	35	0.5	15.5
Developing countries	35	0.7	11

Here, ce, combustion efficiency; TP, total particles; EF(TP), TP emission factor; and BC, black carbon.

2.2. Fossil Fuel Sources

BC emissions from fossil fuel sources mainly result from the burning of diesel fuels and coal used in the domestic sector [*Penner et al.*, 1993]. The emission factors used for the inventory

developed by *Penner et al.* [1993] were 1.91 g C/kg fuel for diesel sources and 5 and 10 g C/kg fuel for coal in the United States and the rest of the world, respectively. These emission factors agree with those used in the recent study by *Cooke and Wilson* [this issue], for the emission from diesel, hard coal, and lignite.

As noted previously, OC concentrations are larger than BC concentrations in urban areas where fossil fuel sources are thought to dominate the emissions of BC concentrations [*Brémond et al.*, 1989; *Cachier*, 1995]. The source of this OC is not necessarily associated with the BC sources noted above [*Gray et al.*, 1984]. However, in order to get a crude estimate of the possible impact of these additional anthropogenic emissions, we used the BC inventory from fossil fuel sources to deduce an OM inventory. Following previous authors [*Pierson and Russell*, 1979; *Rosen et al.*, 1980; *Gaffney et al.*, 1984; *Gray et al.*, 1984; *Cadle and Dasch*, 1988; *Valaoras et al.*, 1988; *Brémond et al.*, 1989], we chose a BC/OC ratio of the order of 30%, a value that is also within the range usually given for fossil fuel combustion. If we assume that total OM is 1.3 times the OC concentration [*Duce*, 1978; *Countess et al.*, 1981], the ratio of OM to BC emissions may be taken as 4.6. Emissions of OM and BC from fossil fuels were assumed to occur with equal intensity throughout the year.

2.3. Natural Sources

The natural emissions of carbonaceous particles from vegetation result from two phenomena: photochemical conversion of the gaseous emissions to species with low vapor pressures, and direct emission of particles from plants [*Cachier*, 1995; *Penner*, 1995]. There are almost no experimental data that can be used to help quantify the latter source, and most emissions are thought to apply to >1 μm diameter. Therefore, in this preliminary inventory, we only considered the secondary formation of carbonaceous aerosols from terpenes. According to *Hatakeyama et al.* [1991], *Pandis et al.* [1991], and *Zhang et al.* [1992], the yield of OC from alpha- and beta-pinene is 0.1 to 8% of their respective mass amounts. This large range is mainly linked to the variability of the initial terpene concentrations, the hydrocarbon to NO_X ratio, and whether the oxidation is initiated by O_3 or OH. We chose a constant factor of 5%, a value within the range determined by *Pandis et al.* [1991], to obtain the OM from the mass of terpenes emitted. The spatial and temporal distributions of the latter emissions were taken from the work of *Guenther et al.* [1995] (C. Atherton, personal communication, 1995). The formation of particles from isoprene was not included because their particle yields under ambient conditions are thought to be negligible [*Pandis et al.*, 1991].

2.4. BC Inventory: Comparison With the Study of *Cooke and Wilson* [this issue]

Cooke and Wilson [this issue] developed a BC emission inventory considering the burning of savanna and forest fires (including both those of the temperate and tropical areas), diesel, coal, fuel wood, and charcoal sources and used this inventory in the 3-D global model Moguntia [*Zimmerman*, et al., 1989]. Compared with our inventory, these authors did not take into account agricultural fires and some domestic fires and the contribution of some countries as Australia and Russia. Like our study, they did not include natural fires in the boreal forests. Although the total emissions from these fires are expected to represent only a few percent of the global inventory [*Penner*, 1995], as shown below, the lack of their inclusion may affect our comparison to data at far northern latitudes. The total BC emissions from the Cooke and Wilson inventory are of the order of 13.5 Tg C/yr, whereas our inventory yields a total of 12.3 Tg C/yr. According to the previously described approximations, the inventory of *Cooke and Wilson* [this issue] would increase somewhat if these sources were included. The fossil fuel sources of BC in the inventory of Cooke and Wilson are distributed geographically using the same method as in this study as well as in the study of *Penner et al.* [1993]. However, a comparison of the relative importance of savanna and forest fires shows that their BC emissions are higher than ours by a factor of 2. In Africa for example, this may be due to the choice of the frequency of burning which is different in the two studies (see section 2.1).

3. Geographical Distribution of BC and OM

3.1. The Grantour Model

The Grantour model is a Lagrangian model of transport, transformation, and removal which uses the wind and precipitation fields of the Community Climate Model (CCM1) [*Williamson and Williamson*, 1987; *Walton et al.*, 1988]. The spatial resolution of the meteorological fields used is approximately 4.5° latitude by 7.5° longitude. The model has 12 vertical levels, with seven in the troposphere and five in the stratosphere.

Briefly, the model treats a set of constant mass air parcels that are advected by the simulated winds interpolated from a fixed Eulerian grid. As noted by *Penner et al.* [1991a,b], the use of 50,000 parcels to represent monthly average concentrations gives reasonable numerical accuracy. Also, following the study of *Penner et al.* [1991b], we use an operator split-time of 6 hours.

The model calculations reported below occurred in two steps. The first year of the simulation started with a clean background atmosphere and was carried out with 25,000 parcels and used a 12-hour operator split time. The second year of the simulation started from the steady atmosphere generated by the first run and used the parcel density number and operator split time mentioned above. Here we report only the results from the second year of the simulation.

The emission of BC and OM by the sources previously described were used as sources in the Grantour model. In addition, the treatment of sulfate aerosols followed that described by *Penner et al.* [1994] and *Chuang et al.* [1994]. Emissions from savanna, forest, and open-fire agricultural fires are known to be injected to the free troposphere as a result of the buoyancy developed by the heat of the fire and by daytime convection occurring in tropical areas. In the model, we inject these sources into the first 2000 m. The fossil fuel, domestic fires, and natural sources are injected into the boundary layer and are therefore distributed between the surface and 1000 m. We took into account both dry and wet deposition, with the latter process dominating particulate removal [*Ducret and Cachier*, 1992]. We chose a dry deposition velocity of 0.1 cm/s. Precipitation scavenging was treated as described by *Walton et al.* [1988] and *Penner et al.* [1991b, 1993]. Wet removal occurs in both convective and stratiform precipitation. The rate of removal R from level k and precipitation type j may be written as follows:

$$R_j(k) = S_j p_j(k)$$

where p is the rate of precipitation in cm/h given by the CCM1 fields and S_j the scavenging coefficient in cm^{-1}. According to

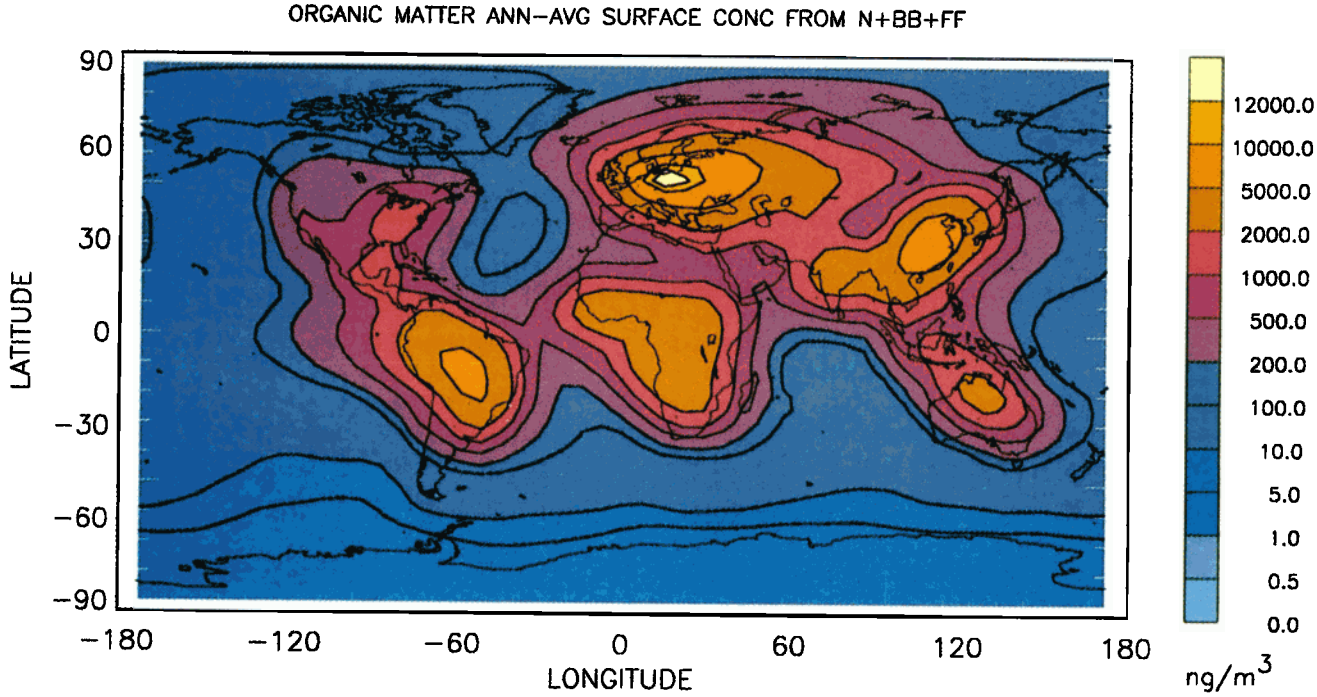

Plate 2. Annual average global distribution of the surface concentrations of organic matter when all sources are included (in ng/m^3).

Penner et al. [1993] and from scavenging ratios given in the literature, we have prescribed a removal coefficient in our model simulations equal to 2.1 cm^{-1} for stratiform precipitation and 0.6 cm^{-1} for convective precipitation. Whereas previous papers have estimated that the BC particles emitted by fossil fuel sources could be more hydrophobic than those emitted by biomass because they initially appear as an external mixture, we assumed a constant value for the BC scavenging ratio for both combustion sources. Indeed, according to *Parungo et al.* [1992, 1994], the BC aerosol emitted by fossil fuel sources may rapidly aquire a coating of sulfate, a feature which would allow the BC to be scavenged as easily as more hydrophilic substances. In addition to the above specifications, large-scale diffusion was assumed to have a horizontal diffusion coefficient of 10^8 cm^2/s. The vertical diffusion coefficient was 10^4 cm^2/s in the troposphere and 10^2 cm^2/s in the stratosphere.

3.2. Results

An overall test of the model simulation is provided by comparing the particle source rate with the total deposition rate. For example, we find a total dry and wet deposition rate for BC of 3.0 and 9.3 Tg/yr, confirming that these are equal to our total yearly source (12.3 Tg/yr) as given in Table 1. The total abundance of black carbon in the atmosphere is calculated to be 0.13 Tg. This, together with the source rate implies a residence time of 4-4.5 days, which is in agreement with the mean values of aerosol lifetime determined by *Lambert et al.* [1982] and *Ogren et al.* [1984]. It is important to note that if we had considered more hydrophobic particles, then their lifetime would be longer.

Plate 2 and Figures 4a and 4b show the annual average and the January and July global distribution of organic matter obtained from the model when all sources are included. To our knowledge, this is the first global simulation of organic particles. Plate 2 shows that the distribution of sources in both hemispheres leads to a particle distribution that is widely spread over the continental areas, but with an abundance that is 10 times higher in the northern hemisphere compared to that of the southern hemisphere. Biomass sources are distributed approximately evenly between the hemispheres in the tropics, while fossil fuel and natural emissions dominate in the northern hemisphere. From

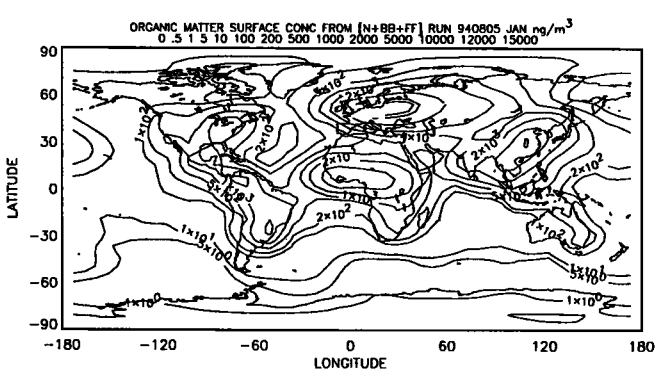

Figure 4a. Same as Plate 2, but for January.

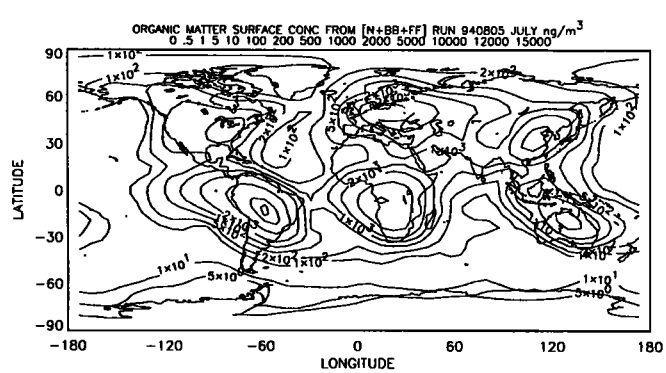

Figure 4b. Same as Figure 4a, but for July.

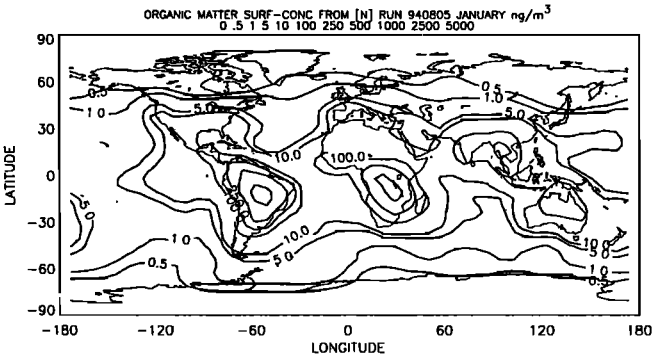

Figure 5a. Global distribution of the surface concentrations of organic matter (in ng/m^3) in January when only the natural source is taken into consideration.

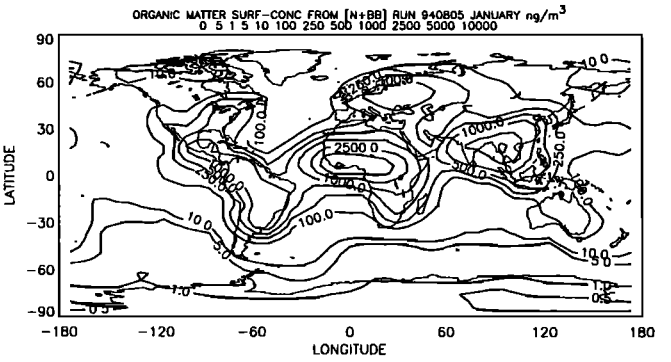

Figure 6a. Global distribution of the surface concentrations of organic matter (in ng/m^3) in January when only the natural source and the biomass burning sources are included.

plots of monthly concentrations (e.g., Figures 4a and 4b), we note that part of the African continent is polluted by particles during each month of the year, a feature already reported from satellite data [*Cahoon et al.*, 1992]. The transport of particles to the tropical Atlantic Ocean due to biomass burning sources in both Africa and South America as noted by *Andreae et al.* [1994] is also evident in these figures.

We examine the relative importance of the sources of natural organic particles in Figures 5a and 5b. The mean organic concentration from the natural sources for the month of July (Figure 5b) represents 2-40% of the July concentrations shown in Figure 4b. Higher ratios correspond to areas which are less influenced by the combustion sources and/or have high terpene emissions. The seasonal variation of emissions is evident from a comparison between the January (Figure 5a) and July (Figure 5b) distributions, especially at middle to high latitudes in the northern hemisphere. As noted there, vegetation emissions are more important during the northern hemisphere summer: indeed, with the larger land mass in the northern hemisphere, the mean global terpene emissions are 1.3 Tg/month in July and only 0.7 Tg in January.

Figures 6a and 6b show the distribution of organic matter surface concentrations when the biomass burning source contribution is added to that of the natural sources from Figures 5a and 5b. The largest concentration of organic particles is situated south of 20N. In January, in Africa, the largest concentration is mainly north of the equator, where the dry season occurs. In July the largest concentration in Africa is south of the equator. As already shown by precipitation studies [*Cachier and Ducret*, 1991], the influence of biomass burning pollutants in the region of Africa north and south of the equator persists throughout the year. Biomass burning in Brazil peaks during the months of July through September, and the largest concentrations appear at that time.

The role of urban and fossil fuel sources may be characterized by comparing the concentrations in Figures 6a and 6b with those in Figures 4a and 4b, which represent the surface concentrations of organic matter emitted by all sources. The addition of organic matter from urban and fossil fuel sources mainly increases the concentrations in the northern hemisphere; those in the southern hemisphere are almost unchanged. The organic particle concentrations due to urban and fossil fuel emissions are larger in central Europe and Asia than in America. This difference is also evident in the predicted distribution of BC surface concentration (see below) and may be linked to the geographical distribution of fossil fuel sources. In the United States, as shown by *Penner et al.* [1993], the diesel fuel sources dominate over other fossil fuel sources, whereas in Eastern Europe, the former USSR, and Asia, domestic and commercial coal sources dominate. The emission factors that we used for BC from coal combustion are more than a factor of 2 higher than those used for diesel combustion. Finally, we note that our fossil fuel inventories are based on FAO data for the year 1980. Consequently, if the use of coal in central Europe has declined during the 1990s, the model OC concentrations for these locations would be higher than current observations might indicate.

Figures 7a and 7b show the predicted surface concentration of BC from all sources. By comparing Figures 4a and 4b for OM with Figures 7a and 7b, we note that the model-predicted carbonaceous particles in the north polar region have a fossil fuel

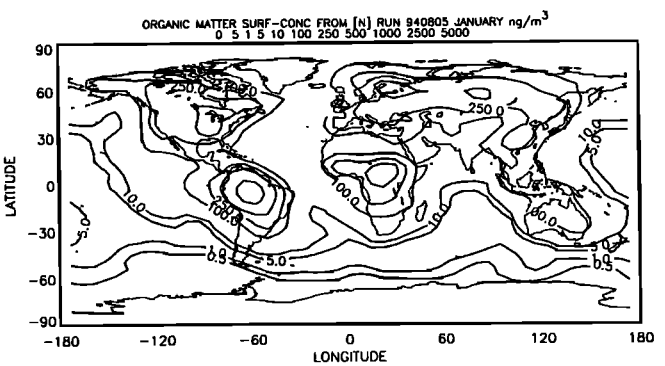

Figure 5b. Same as Figure 5a, but for July.

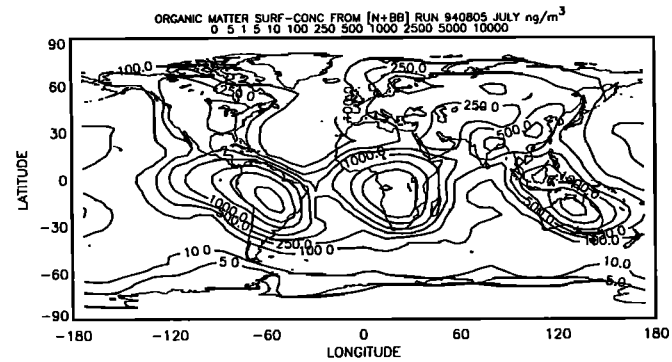

Figure 6b. Same as Figure 6a, but for July.

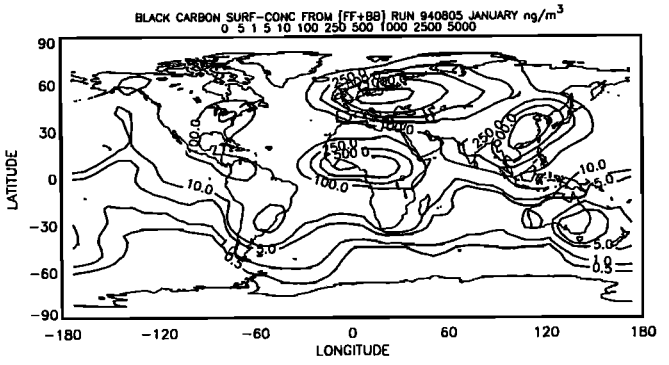

Figure 7a. Global distribution of the surface concentration of black carbon particles (in ngC/m^3) in January when all sources are included.

origin, whereas those near the south pole have a biomass burning origin. In the north pole, meteorological processes act to produce higher concentrations of these particles in January than in July (in keeping with the Arctic haze phenomenon). We also note that the concentrations of BC near the south pole are larger in July than in January, a feature which is mainly explained by the seasonal variability of the biomass burning sources in the southern hemisphere.

3.3. Sensitivity Tests

The results reported in the previous paragraphs are strongly dependent on parameterizations that we have chosen in the Grantour model, particularly those that govern the aerosol residence time. Here we examine the sensitivity of our results to the height of injection and the precipitation scavenging coefficient.

Figure 8a presents the sensitivity of simulated BC surface concentrations to a variation of the atmospheric injection height. Here, we compare the surface concentration calculated by the model using the boundary conditions previously described with the concentrations obtained when all the sources are introduced in the first 1000 m. Close to the sources, the increase of the injection height produces a small decrease of the surface concentrations (less than 20%). However, as shown in the figure, the height of injection has an important impact on the simulated concentrations at remote sites. Indeed, if the injection of particles takes place at a higher altitude, larger concentrations are predicted for very remote sites (indicated by the lowest concentrations). Concentrations lower than 50 ng/m^3 may be changed by a factor of 2.

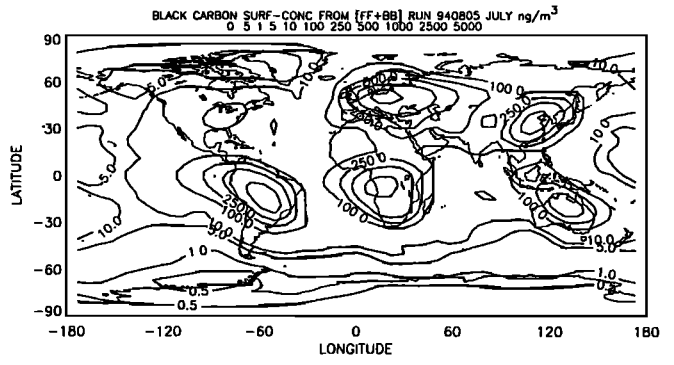

Figure 7b. Same as Figure 7a, but for July.

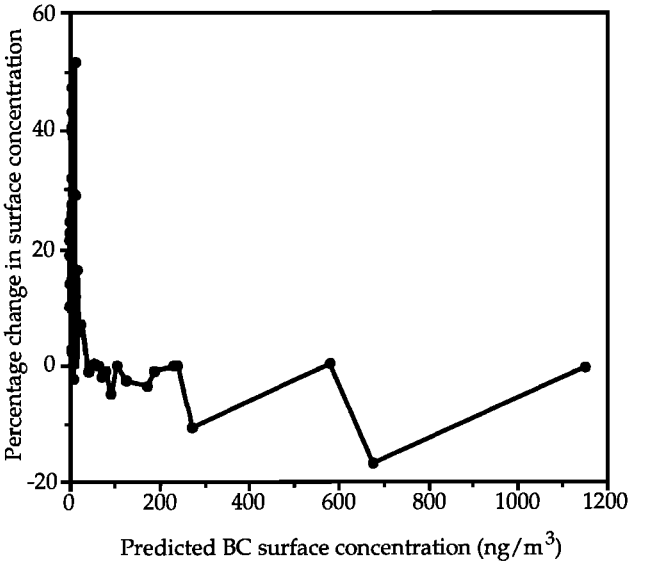

Figure 8a. Sensitivity test showing percentage change in predicted BC concentrations between a simulation with the standard injection heights and a simulation in which all sources were injected into the lowest 1000 m.

We also tested the sensitivity of the aerosol surface concentrations to variations about the mean values of the scavenging coefficients used here, namely, 2.1 and 0.6 cm^{-1} for stratoform and convective precipitation, respectively. These coefficients are based on observed scavenging ratios. However, observations of scavenging ratios vary widely [see *Penner et al.*, 1993]. Figure 8b presents the sensitivity of the BC surface concentrations to a ±15% change in the scavenging coefficients. If the scavenging coefficients are decreased, the aerosols are transported further because there is less removal by precipitation. Because concentrations near the source are mainly determined by the local source rate and their rate of removal by advection, they

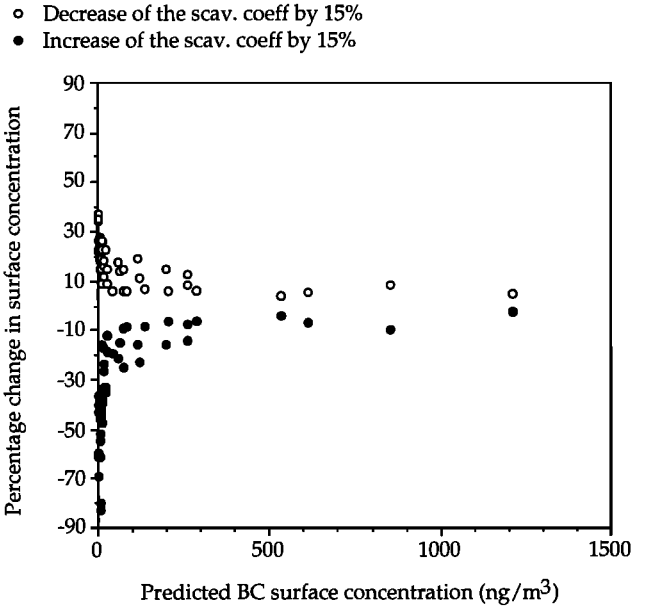

Figure 8b. Sensitivity test showing percentage change in predicted BC concentrations for a simulation in which the scavenging coefficients are increased (solid circles) and decreased (open circles) by 15%.

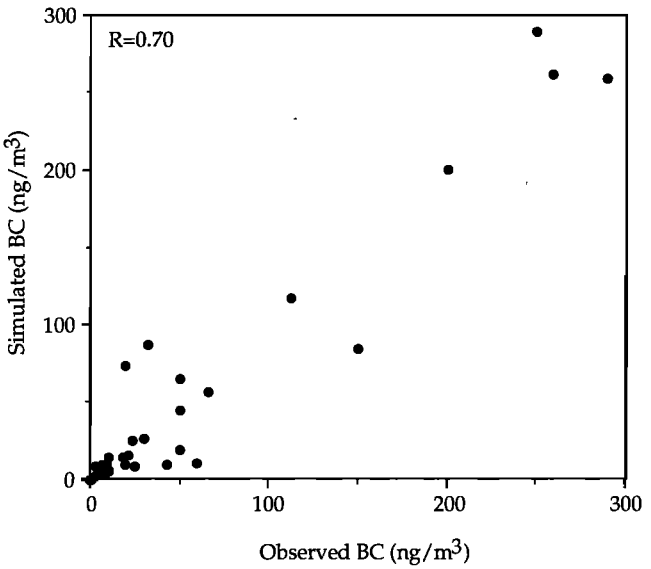

Figure 9. Scatter plot of predicted and observed black carbon surface concentrations at sites whose concentrations are less than 300 ng C/m^3.

are not very sensitive to a change in scavenging coefficients. On the other hand, air parcels in locations far from sources have been subjected to many rainfall events since leaving the source area. Hence they are more sensitive to the scavenging parameters. In Figure 8b, remote locations are represented by parcels with small concentrations. The figure shows that remote-area concentrations may be increased by between 1 and 40% with a decrease in the scavenging coefficient of 15%. Of course, it is important to note that the BC wet deposition is decreased as well. Increasing the scavenging coefficient by 15% generated a decrease of remote surface concentrations by between 1 and 40%. The range of parameter variation chosen here, ±15%, is well within the range of the scavenging ratios usually given in literature data. Because the surface concentrations at remote sites are extremely sensitive to this coefficient, it is clear that models for global transport would greatly benefit from an improved description of the wet removal process.

4. Comparisons With Observations

4.1. Carbonaceous Aerosols in the Atmosphere

The accuracy of the inventories and the model formulation were tested by comparing the model simulations of carbonaceous aerosols with observations. We collected experimental data on BC concentrations from a literature survey and found data for more than 50 locations. These represented data from both short-term measurements (during a campaign for example) and long-term measurements (monthly or annually averaged). Figure 9 presents a scatter plot of observed and simulated concentrations of BC from those sites whose measured concentration is less than 300 ng/m^3, while Tables 4a–4c give a detailed comparison by location. Figure 9 demonstrates that there is no overall bias in the model results. As shown in Table 4a, the simulated and observed BC surface concentrations are in general agreement in the Pacific and Atlantic Oceans. Because the observations are often single measurements, for a single time period, we do not expect the model, which represents a climatological average, to precisely reproduce the observations. These comments apply to the measurements taken in the Sargasso Sea, a few points in the Pacific Ocean, and at Enewetak. However, the observations reported for Mauna Loa represent a long-term pattern [*Bodhaine,* 1995]. We note that at this sampling location (situated at 3500-m altitude), both the annual means and the monthly means compare favorably.

In Table 4a, comparison of the model results with observations by *Parungo et al.* [1994] indicates that there may be a systematic overprediction by the model for some points off the Asian coast. However, we note that the concentrations in source regions in Asia are, if anything, underpredicted (compare Table 4b]) It is important to better quantify both the sources and concentrations

Table 4a. Comparison of the Simulated and the Observed Black Carbon Surface Concentrations at Sites in the Pacific and Atlantic Oceans

Location	Time Period	BC Concentration, ng C/m^3 Observed	Simulated	References
	Atlantic Ocean			
68N, 8W (Northeast Atlantic)	Annual	112	117	*Jennings and O' Dowd* [1990]
42.5N 14W	October	40-60	44.3	*Andreae et al.* [1984]; *Cachier et al.* [1990]
32.2N, 64.45W (Bermuda)	Annual	30	27	*Wolff et al.* [1981]
30N, 50W (Sargasso Sea)	July	60	11	*Chesselet et al.* [1981]
20S, 40W	October	20	74	*Andreae et al.* [1984]
	Pacific Ocean			
40-50N, 160W	May, June, July	20	10	*Andreae et al.* [1984]; *Clarke* [1989]
10-30N, 160W	Oct., Nov., Dec., May, June, July	7	6.6	*Andreae et al.* [1984]; *Clarke* [1989]
0, 160W	Annual	3	2.95	*Andreae et al.* [1984]; *Clarke* [1989]
10-30S, 160W	Oct., Nov., Dec., May, June, July	8	4	*Andreae et al.* [1984]; *Clarke* [1989]
19.3N, 155.4W (Mauna Loa)	Annual	7.5	9.3	*Bodhaine et al.* [1995]
19.3N, 155.4W (Mauna Loa, 3500 m)	Annual	12.3	11	*Clarke* [1989]
0, 120W (equatorial Pacific)	June	10	14	*Andreae et al.* [1984]
27-32N, 127-129E	April, May	355	639	*Parungo et al.* [1994]
27-33N, 124-129E	Oct., Nov.	505	1008	*Parungo et al.* [1994]
28-32N, 125-128E	Dec.	133	1233	*Parungo et al.* [1994]
10N, 165E	July	25	9	*Parungo et al.* [1994]
11.3N, 162.1E (Enewetak)	April	50	20	*Cachier et al.* [1990]
10N, 113E (China Sea)	June	33	87	*Parungo et al.* [1994]
0, 150E (western Pacific Ocean)	July	9	10	*Parungo et al.* [1994]
13.6S, 172W (Samoa)	July	19	14	*Cachier et al.* [1986]

Ranges refer to the minimum and maximum observed values.

Table 4b. Comparison of the Simulated and the Observed Black Carbon Surface Concentrations at Rural Sites

Location	Time Period	BC Concentration, ng C/m^3 Observed	Simulated	References
		Northern Hemisphere		
53.3N, 9.8W (Mace Head)	Annual	48-289	259	*Jennings et al.* [1993]
28N, 82W (Florida)	Annual	400	136	*Andreae et al.* [1984]
34.3N, 106W (Southwest)	Annual	150-220	84	*Andreae et al.* [1984]; *Pinnick et al.*, 1994]
35.3N, 80W (North Carolina)	Annual	520	202	*Andreae et al.* [1984]
68.2N, 18.3E (Abisko)	Annual	259-780	262	*Clarke* [1989]
52.4N, 1.4E (Hemsby)	April	466	1210	*Yaaqub et al.* [1991]
41.4N, 42.5E (Abastumani)	Annual	980	729	*Dzubay et al.* [1984]
36.2N, 133.2E (Dogo)	Annual	623	612	*Mukai et al.* [1990]
38.35N, 68.48E (Isenbai Village)	Jul.-Sept.	1000	454	*Parungo et al.* [1994]
40N, 116E (Beijing Rural)	Jul.-Sept.	1710	1127	*Parungo et al.* [1994]
30.5N, 119.5E (Lin An Station)	Jul.-Sept.	2070	1596	*Parungo et al.* [1994]
		Southern Hemisphere		
2S, 77.3W (Ecuador)	Annual	100-520	289	*Andreae et al.* [1984]
10S, 55W (Brazil)	Annual	200-620	536	*Andreae et al.* [1984]
10S, 76W (Peru)	April	24	25.5	*Cachier et al.* [1986]
40.7S, 144.4E (Cape Grim)	Annual	3	8 .9	*Heintzenberg and Bigg* [1990]

Ranges refer to the minimum and maximum observed values.

in Asia. The long-term record of concentrations at Mauna Loa could then serve to constrain the treatment of precipitation scavenging in the model because of the sensitivity of the model results to precipitation scavenging coefficients noted in the previous section. Comparison of this version of the model with those from an Eulerian version shows that the high concentrations off the Asian coast in the model may result from the smoothing that occurs in mapping the concentrations on the parcels in the model to concentrations at a location on the grid. In this procedure, all parcels within a 10° great circle around a given location contribute to the concentration reported at that locale, although the more distant parcels contribute with less weighting [*Walton et al.*, 1988]. Hence, at a coastline, concentrations from the continental source regions can contribute to the smoothed concentration at a grid point off the continent.

Table 4b compares the model results for black carbon with observations in semi-urban or rural locations of the northern and southern hemisphere. Both Mace Head and Cape Grim are coastal sites and may be impacted by the mapping procedure noted above. Because sampling protocols at these sites normally discriminate against polluted air coming directly off the coast, we report the computed concentrations from a grid box that is one zone away from the actual sampling site. Thus for Mace Head we report the concentration at 53.3N, 12.8W instead of 53.3N, 9.8W, and for Cape Grim we report 45.4S, 144.4E instead of 40.7S, 144.4E.

Table 4c presents a comparison between the observed and simulated BC concentrations in remote areas. In contrast with the model results of *Cooke and Wilson* [this issue], our model is in reasonable agreement with these data, a feature that probably results from the higher resolution of our model and our accurate treatment of advection. Long-term measurements exist for a few remote sites in the southern and northern hemispheres. These include Amsterdam Island, South Pole, and Barrow. Figure 10a shows a comparison of model results and monthly average observations for 1991, 1992 and 1993 for Amsterdam Island. At this location the model and observations are in good agreement, demonstrating that the magnitude and timing of emissions from southern Africa are quite good. However, it is clear that the interannual variations shown by the experimental data cannot be reproduced by the model which uses a single year's meteorological fields and our best estimates for average emissions. The comparison of the model results and observations at the South Pole (Figure 10b) is not as good. The model is able to reproduce the increase in BC concentrations beginning in June, but the highest concentrations are not reproduced. At Barrow (Figure 10c), the model shows a slight seasonal variation whose timing agrees with the timing of the Arctic haze phenomenon, but

Table 4c. Comparison of the Simulated and the Observed Black Carbon Surface Concentrations at Remote Sites

Location	Time Period	BC Concentration, ng C/m^3 Observed	Simulated	References
		Northern Hemisphere		
70N, 40W (Greenland)	July	30	10	*Cachier* [private communication, 1995]
71.2N, 156.3W (Barrow)	Annual	43	10	*Bodhaine* [1995]
74N, 25E (Arctic Point)	Winter	70-225	119-200	*Heintzenberg* [1982]
79N, 12E (Spitsbergen)	Annual	66	57	*Heintzenberg and Leck* [1994]
82.5N, 62.5W (Alert C.)	Summer	10-20	6.4	*Hopper et al.* [1991]
	Winter	50-100	19	*Hopper et al.* [1991]
		Southern Hemisphere		
37.5S, 77.3E (Amsterdam Isl.)	Annual	5.5	4.5	*Cachier et al.* [1994]
41S, 174E (New Zealand)	August	22	15.2	*Cachier et al.* [1986]
75.4S, 27W (Halley Bay)	Annual	0.3-3	0.34	*Cachier et al.* [1986]; *Hansen et al.* [1988]
87S, 102W (South Pole)	Annual	0.3	0.16	*Hansen et al.* [1988]
87S, 102W (South Pole)	Annual	1.3	0.16	*Bodhaine* [1995]

Ranges refer to the minimum and maximum observed values.

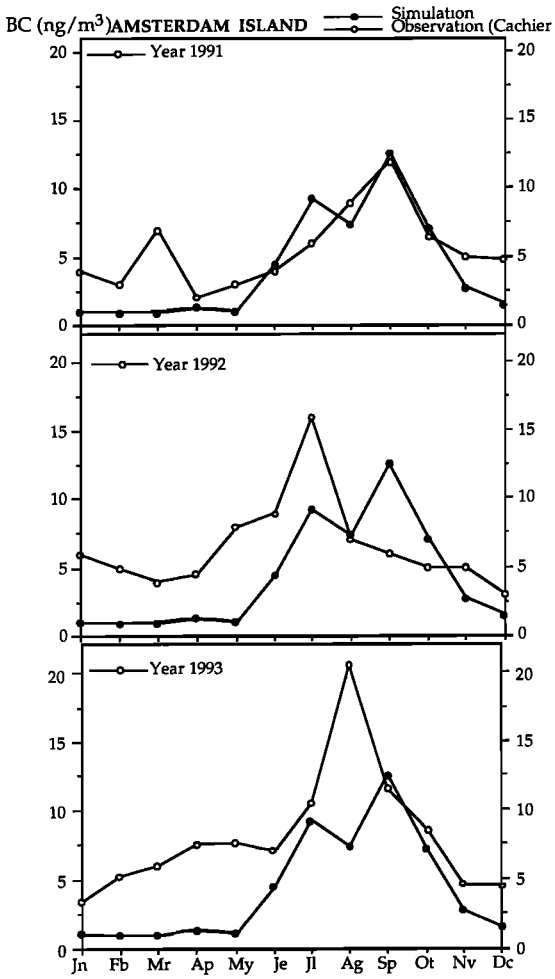

Figure 10a. Comparison of the simulated black carbon surface concentrations (in ngC/m^3) with observed data at Amsterdam Island.

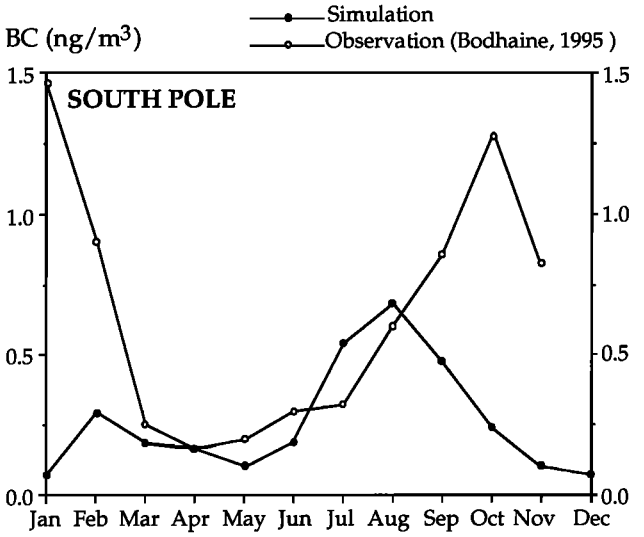

Figure 10b. Same as Figure 10a, but for the South Pole.

the model concentrations are again much lower than the observations. The underprediction in the polar regions may result from either (1) underestimation of biomass sources, (2) overestimation of precipitation scavenging, or (3) poor representation of advection by the underlying climate model toward the polar regions. We cannot, at this time, distinguish between the three possible reasons for discrepancies between the model and observations in both the South Pole and at Barrow. In summer, the low concentrations at Barrow may result from the fact that we have not included the sources of carbonaceous aerosols from natural fires which are small on a global basis [e.g., *Penner*, 1995] but may contribute to the observed concentrations at this site (compare the data for Greenland in Table 4c). The large discrepancy in Figure 10c between the modeled and observed BC concentrations in winter in Barrow may also be due to a poor representation by our model of the Arctic boundary layer. Further work is needed to resolve these issues.

Figures 11a and 11b show a comparison of model predicted concentrations and observations of BC and OM from the Improve network in the United States [*Cahill et al.*, 1990; *Malm et al.*, 1994]. The model appears to be systematically lower than these observations. It is also lower than the observations of BC in the United States reported by *Andreae et al.* [1984] (Table 4b). We note that the measurements reported by *Andreae et al.* [1984] refer to 1983 while those for *Malm et al.* [1994] refer to 1988-1991. The inventory we used here (which dominates the BC concentrations in the United States was developed for 1980 (FAO), and some growth in usage could be assumed to have occurred since then. We may note that the BC inventory for fossil fuel emissions from North America given by *Cooke and Wilson* [this issue] is approximately 4 times larger than the inventory used here. We conclude that uncertainties in inventory could easily explain the discrepancy between observed and simulated BC concentrations in the United States. Alternatively, scavenging by precipitation may be systematically overestimated in this region (see below). These factors may also explain our systematic underprediction of OM in the United States (Figure 11b).

Table 5 shows a comparison between observed and simulated OC concentrations. There are very few measurements of OC reported in the literature. However, the model results are in reasonable agreement with the data, especially at Mace Head, Puerto Rico, and Mauna Loa. More definitive statements

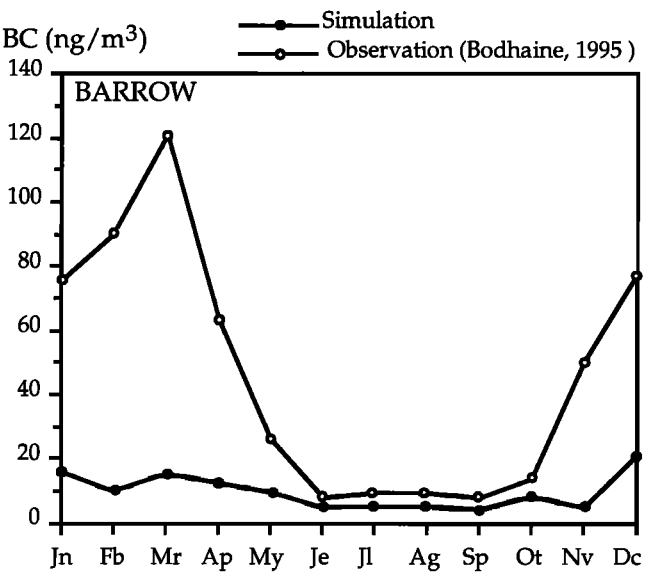

Figure 10c. Same as Figure 10a, but for Barrow, Alaska.

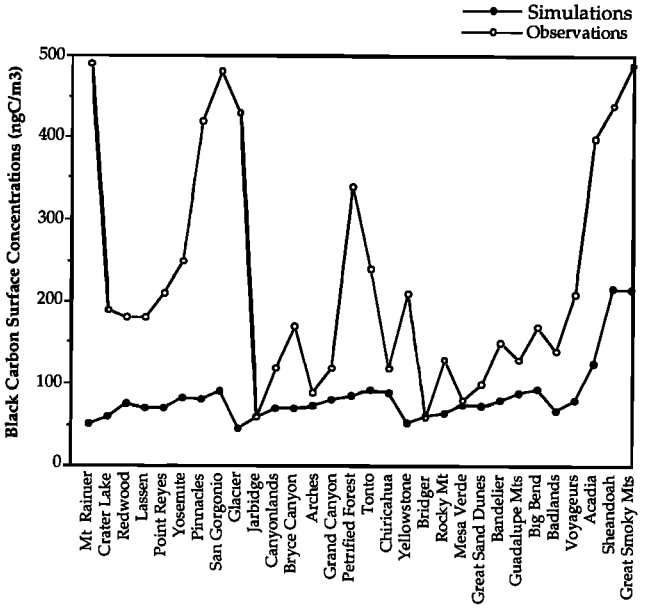

Figure 11a. Comparison of the predicted and observed surface concentrations of black carbon particles (ng C/m^3) in North American rural sites (Improve experiments [*Cahill et al.*, 1990; *Malm et al.*, 1994]).

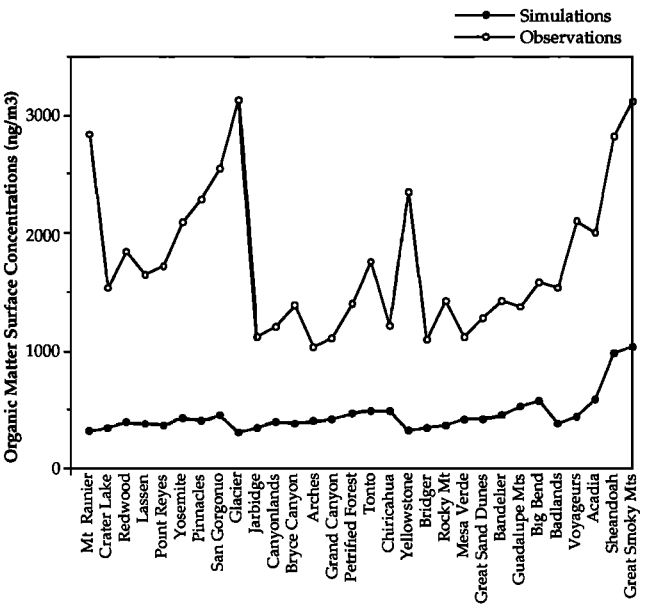

Figure 11b. Same as Figure 11a, but for organic matter (ng/m^3).

regarding the quality of this simulation require a better understanding of OC sources from vegetation as well as OC sources associated with fossil fuel emissions and urban activity.

Figure 12 shows a comparison between model predictions and experimental data reported by *Andreae et al.* [1994] of the vertical profile of the total particle concentration in ng/m^3. These observations refer to a location and time when biomass burning was predominant. The model-simulated profile decreases monotonically from values at the surface, while the observations show an increase above the surface. We do not expect the model to reproduce features such as these because of its rather simplified representation of the boundary layer. On the other hand, the good agreement at higher altitudes demonstrates that vertical transport is approximately correct. This was shown previously in the discussion of the comparison of the model to observations at Mauna Loa, a site located at 3500-m altitude.

Figures 13a and 13b show the annually averaged and zonal average concentrations of OM and BC, respectively, from all sources. Near-surface concentrations of both components are largest at northern midlatitudes, reflecting the importance of fossil fuel sources, while the peak concentrations in equatorial regions follow from the biomass burning sources. Concentrations

Table 5. Comparison of the Simulated and Observed Surface Concentrations of Organic Carbon in Rural and Remote Sites of the Northern and Southern Hemispheres

		OC Concentration, ng C/m^3		
Location	Time Period	Observed	Simulated	References
		Northern Hemisphere		
11.3N, 162.1 (W Enewetak)	April-May	700	70	*Chesselet et al.* [1981]
20N, 157.5W (Mauna Loa)	Annual	50	48	*Clarke* [1989]
30N, 50W (Sargasso Sea)	July	440	63	*Chesselet et al.* [1981]
53.3N, 9.8W (Mace Head)	Annual	1024	927	*Cachier et al.* [1994]
36.15N, 133.2W (Oki Island)	Annual	1417	1107	*Mukai et al.* [1990]
41.4N, 42.5E (Abastumani)	July	2000	1710	*Dzubay et al.* [1984]
33.15N, 119.3E (San Nicolas Island)	Oct.-Nov.	524	470	*Hidy et al.* [1974]
18.2N, 62.5W (Puerto Rico)	March	500	660	*Novakov and Penner* [1993]
70N, 40W (Greenland)	Dec.	158	232	*Cachier* [private communication, 1995]
32.2N, 64.45W (Bermuda)	Annual	150-470	226	*Hoffman and Duce* [1974]
42.5N, 14W (North Atlantic)	Oct.-Nov.	175.5	280-390	*Ketsediris et al.* [1976]; *Andreae* [1983]
15N, 27W (North Atlantic)	Nov.	384	330-1600	*Ketsediris et al.* [1976]; *Andreae* [1983]
1.6-5.5N, 81W (Pacific)	Feb.	417	425	*Wolff et al.* [1986]
		Southern Hemisphere		
37.5S, 77.3E (Amsterdam Isl.)	Annual	22	27.4	*Cachier et al.* [1994]
41S, 174E (New Zealand)	August	130	81	*Cachier et al.* [1986]
2S, 77.3W (Ecuador)	Annual	510	406-5000	*Andreae et al.* [1984]
10S, 76W (Peru)	March-April	160	385	*Cachier et al.* [1986]
13.55S, 172W (Samoa)	Aug.	59	52	*Cachier et al.* [1986]
40.7S, 144.7E (Cape Grim)	Annual	230	50-127	*Andreae* [1983]
20S, 40W (South Atlantic)	Oct.-Nov.	538	280	*Andreae et al.* [1984]
2.4-0S, 81W (Pacific)	Feb.	242	152	*Wolff et al.* [1986]

Ranges refer to the minimum and maximum observed values.

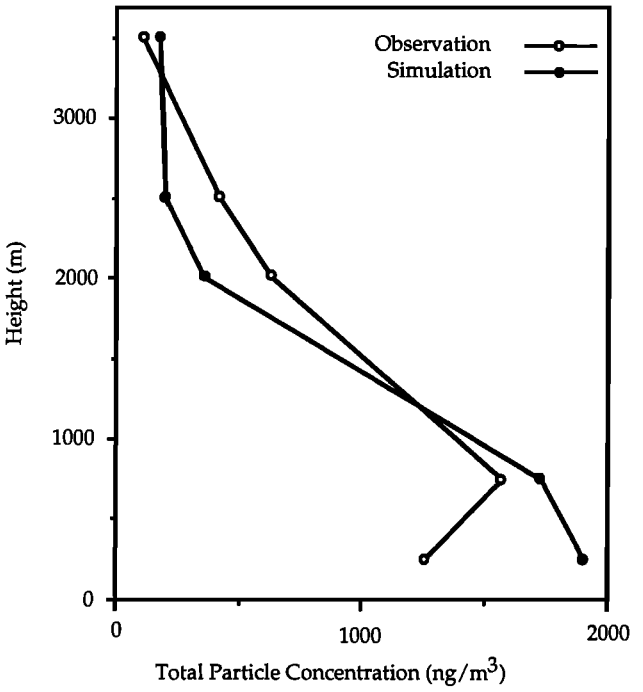

Figure 12. Comparison of the predicted and observed [*Andreae et al.*, 1994] vertical distribution of the total particle concentration in ng/m^3.

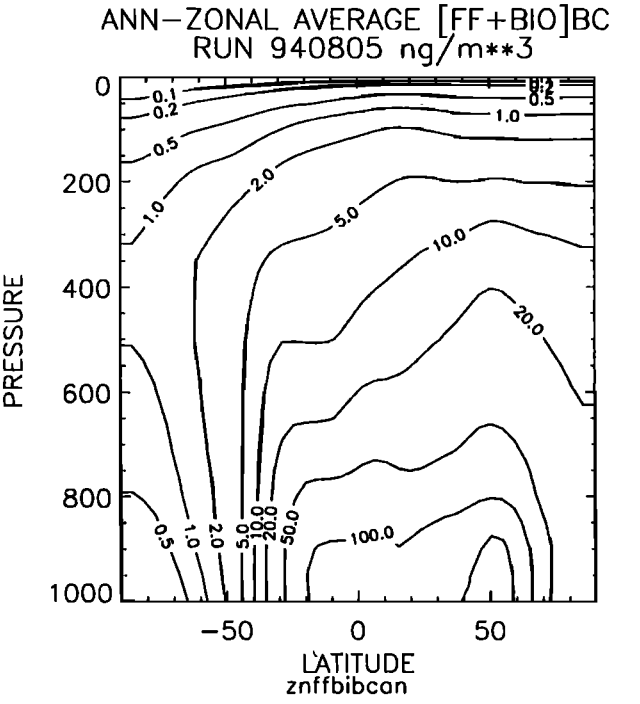

Figure 13b. Same as Figure 13a, but for concentrations of black carbon (in ng C/m^3).

drop rapidly with height. At northern midlatitudes, near 250 mbar, predicted concentrations of BC are between 5 and 10 ng/m^3. These concentrations are similar in magnitude to the concentrations of fresh soot measured in aircraft flight corridors [*Blake and Kato*, 1995]. Accordingly, this model predicts that the ground-level sources of soot are as important as local sources in determining concentrations in the upper troposphere.

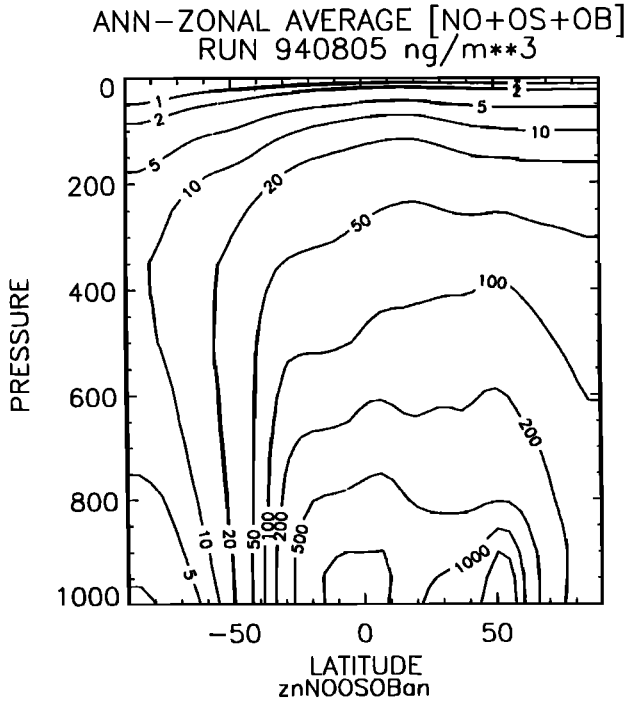

Figure 13a. Predicted annual average and zonal average concentrations of organic matter (in ng/m^3).

4.2. Deposition of Black Carbon

Figures 14a and 14b show the annual average dry and wet deposition of BC, respectively. Dry deposition follows the pattern of surface BC concentrations shown by Figures 7a and 7b. Indeed, the spatial and temporal distributions of both concentrations and dry deposition are governed by local source strength and wind velocity. On the other hand, wet deposition is greatly influenced by the precipitation intensity and frequency. Thus the global pattern of Figure 14b is very different from that of Figure 14a.

As mentioned previously, the removal of BC from the atmosphere occurs mainly through scavenging by precipitation. Thus a comparison of Figures 14a and 14b shows that wet deposition is at least 4 times larger than dry deposition in most locations. Only a few papers have reported the BC concentration in precipitation. This information is usually given in mass of BC per volume of precipitation (μg/L). To compare to these data, the model-simulated values of BC wet deposition given in mass of

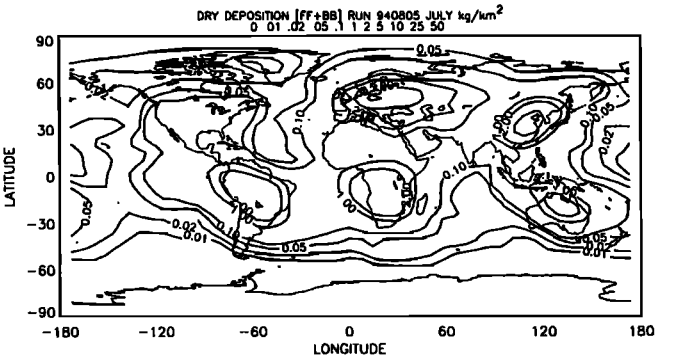

Figure 14a. Global distribution of the dry deposition of black carbon when all the sources are included (in kg C/km^2/month).

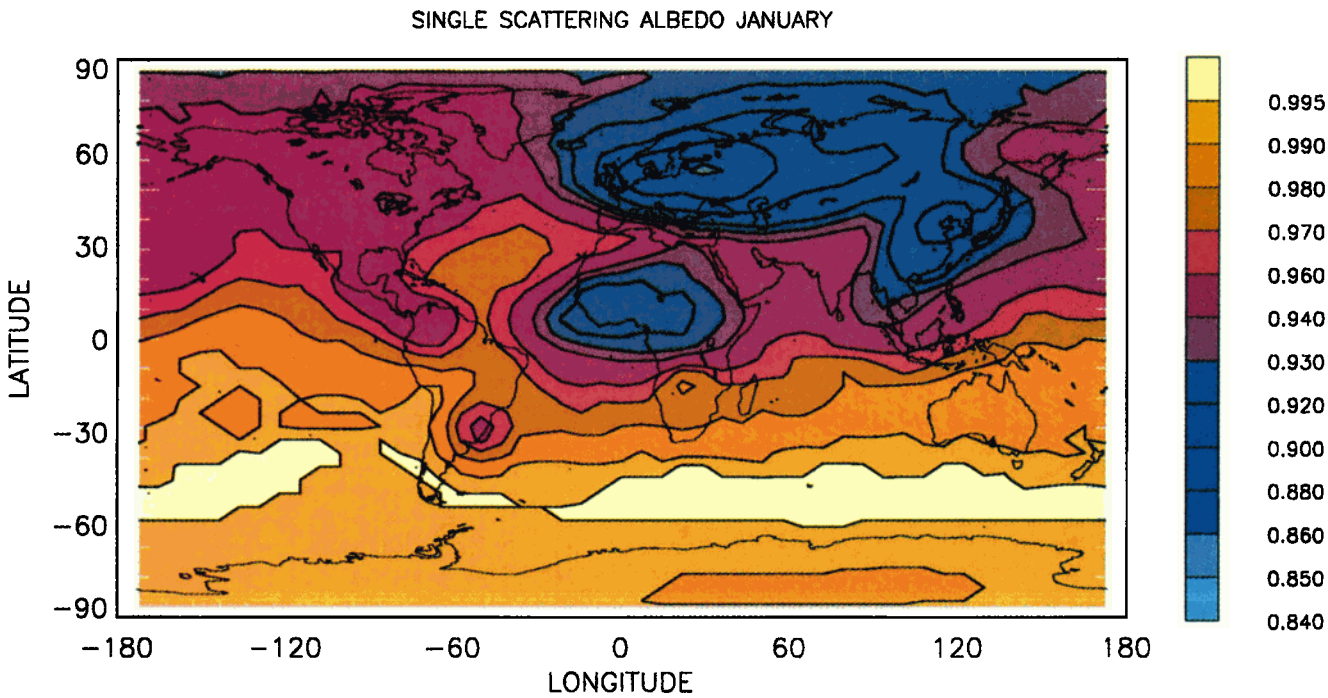

Plate 3a. Global distribution of single scattering albedo values in January, calculated from the model.

BC per unit area (kg/km^2) had to be scaled, taking into account the amount of precipitation at each site. We used two sets of precipitation data for this scaling, the first one given by *Bryson and Hare* [1974] and the second one by the precipitation fields predicted by the general circulation model (GCM) [*Walton et al.*, 1988]. The two results were quite similar except for a few places in North America. For example, the amount of precipitation given by the GCM was 5 times higher than that of *Bryson and Hare* [1974] in El Paso, White Sands Missile Range (WSMR), and Aguirre. Thus some of the poor comparison with data in North America (see below) probably results from its poor precipitation fields.

Table 6 shows the observed and predicted BC in precipitation at a number of different locations throughout the world. As noted above, the predicted concentrations in El Paso, WSMR, and Aguirre are too high by at least a factor of 5, owing at least in part to the GCM's precipitation fields at these sites. Additionally, it is possible that some BC particles, especially those associated

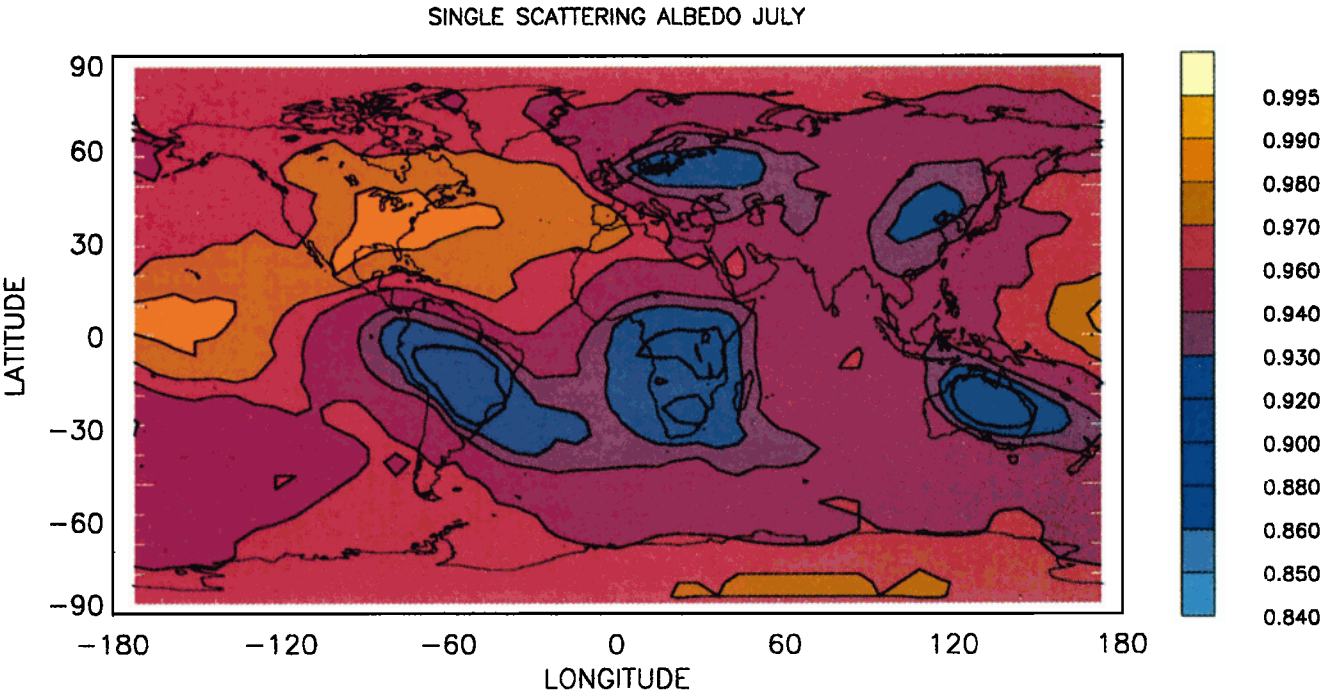

Plate 3b. Same as Plate 3a, but for July.

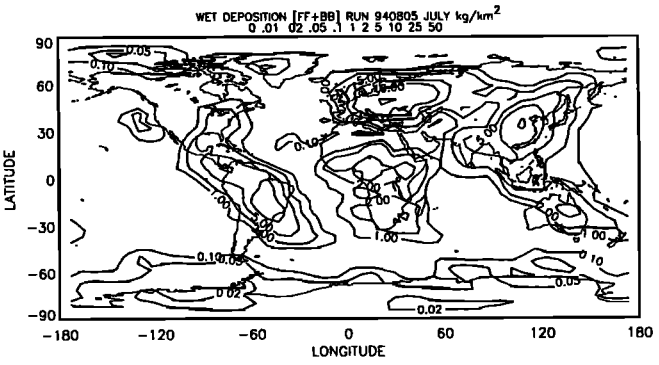

Figure 14b. Same as Figure 14a, but for wet deposition.

with fossil fuel sources, would not yet be associated with sulfur and other components that would render them hydrophilic. Hence our treatment may overestimate scavenging near source regions. This latter reason may also partly explain the systematic underprediction of BC that we obtained when comparing to the U.S. sites in the Improve network [*Malm et al.*, 1994]. As shown in Table 6, however, the model compares reasonably (within about a factor of 2) with observations from other locales throughout the world. Figure 15 compares the monthly average concentrations with observations reported by *Cachier and Ducret* [1991] for Enyele. These authors note that this site is contaminated by biomass smoke throughout the year, a feature that is also seen in the model.

While the above results are encouraging, it is clear that more observations of longer duration would be needed to provide a more stringent test of the model. Improvement in the GCM's treatment of precipitation is probably also needed.

4.3. Aerosol Single Scattering Albedos

We have also tested the model formulation by comparing simulated and observed single scattering albedos (ω_0). The single scattering albedo is defined as the ratio of light scattering to total light extinction by aerosols and is relevant to our study because observations of single scattering albedo are sensitive to the fraction of absorbing (e.g., BC) and scattering (e.g., organic carbon and sulfates) material in the aerosol. We calculated the single scattering albedo as follows:

$$\omega_o = \frac{\sigma_s(BC)\times[BC]+\sigma_s(OM)\times[OM]+\sigma_s(Su)\times[Su]}{\sigma_a(BC)\times[BC]+\sigma_s(BC)\times[BC]+\sigma_s(OM)\times[OM]+\sigma_s(Su)\times[Su]}$$

where [BC] and [OM] represent the BC and OM abundances (in g/m^2). [Su] is the aerosol sulfate abundance calculated by the model (see *Penner et al.* [1994] for a description of this simulation). For this comparison the aerosol carbon and sulfate abundances are calculated for a simulation in which both anthropogenic and natural sources of each component are included. Here, $\sigma_S(BC)$, $\sigma_S(OM)$ and $\sigma_S(Su)$ are the specific scattering cross sections in m^2/g of the BC, OM and sulfate particles, respectively, while $\sigma_a(BC)$ is the specific absorption cross section of BC. Table 7 presents the values of these parameters chosen for our study. We note that our calculation of ω_0 refers to an external mixture of BC, OC, and sulfates. A number of authors have calculated specific cross sections for BC [*Twitty and Weinman*, 1971; *Roessler and Faxvog*, 1979; *Jennings and Pinnick*, 1980; *Japar et al.*, 1984; *Dobbins et al.*, 1994; *Pueschel et al.*, 1994, and S.G. Jennings, personal communication, 1995]. The average values indicated in Table 7 for the near-UV, visible, and near-IR wavelengths are consistent with these studies. We used a constant value for the BC absorption cross section even though a previous study [*Liousse et al.*, 1993] has shown that this coefficient may be strongly dependent on the physical and chemical properties of the aerosols and, consequently, on the different sources. Also, as presented by *Fenn and Oser* [1965] and *D'Almeida et al.* [1991], the particle size of the BC particles, their shape, and consequently, their optical properties may be modified by an increase of the relative humidity; however, here we simply treat the BC optical properties as independent of humidity. There are not many studies which report calculations of the scattering and absorption properties of organic matter. *Holben et al.* [1991], *Sloane* [1983,

Table 6. Comparison Between the Simulated and Observed Black Carbon Concentration in Precipitation for Different Sites

		BC Concentration, µg/L		
Location	Time Period	Observed	Simulated	References
		Northern Hemisphere		
2.8N, 18.1E (Enyele)	Annual	73	53.6	*Ducret and Cachier* [1992]
53.3N, 12.8W (Mace Head)	Annual	30	33	*Ducret and Cachier* [1992]
71.3N, 156.6W [Barrow)	April	23	27	*Clarke and Noone* [1985]
79N, 12E (Spitsbergen)	Annual	31	26	*Clarke and Noone* [1985]
68.3N, 18.5E (Abisko)	April	33	40	*Clarke and Noone* [1985]
77.2N, 61.15W (Greenland)	Annual	2.5	10	*Clarke and Noone* [1985]
65.2N, 43.8W (Dye 3)	Annual	9	7.9	*Chylek et al.* [1987]
55-64N, 10-20W	April-Aug.	70-300	111-330	*Ogren and Charlson* [1984]
82.5N, 62.5W (Alert)	Nov.-Dec.	19	18	*Clarke and Noone* [1985]
79.75N, 4.2W (Greenland Sea)	July	63	46	*Clarke and Noone* [1985]
48N, 123.5W (Hurricane)	March	14.6	11	*Clarke and Noone* [1985]
32.2N, 106.5W (Las Cruce)	Annual	16.5	10.2	*Chylek et al.* [1987]
31.45N, 106.3W (El Paso)	April	16	167.1	*Chylek et al.* [1987]
32.23N, 106.3W (WSMR)	March-April	16.7	127.8	*Chylek et al.* [1987]
34.3N, 106W (Aguirre)	Annual	11.5	93.3	*Chylek et al.* [1987]
32.6N, 105.4W (Cloudcroft)	Annual	4.8	18	*Chylek et al.* [1987]
31.1N, 105.2W (Sierra Blanca)	Annual	4.9	27.8	*Chylek et al.* [1987]
		Southern Hemisphere		
75.92S, 83.92W (Siple Point)	Annual	2.5	2.6	*Chylek et al.* [1987]
90S, 24.8W (Amundsen Point)	Annual	0.35	0.01	*Warren and Clarke* [1990]
75.7S, 27W (Halley Bay)	Feb.-March	18	3	*Clarke and Noone* [1985]

Range given for annual averages includes minimum and maximum values which have been found per year by authors.

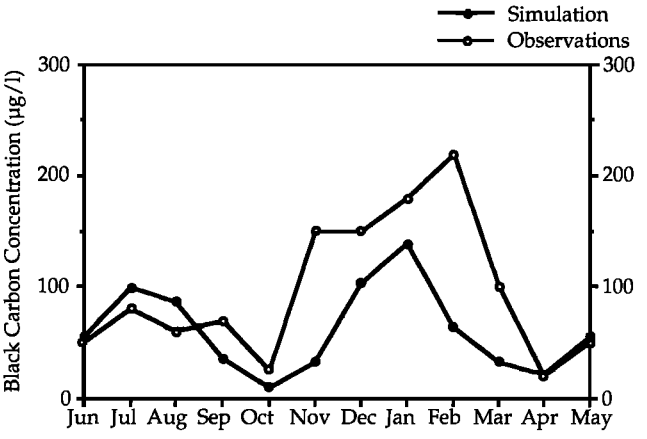

Figure 15. Comparison between simulated and observed black carbon concentration in precipitation (in µg/L) in Enyele, Congo.

1984], and (C. Liousse et al., Remote sensing of carbonaceous aerosol production by African savanna biomass burning, submitted to *Journal of Geophysical Research*, 1995) calculate the light scattering properties of organic matter, assuming a refractive index of the order of 1.43-0.0035i at 0.55 µm, a coefficient close to that of sulfate aerosols. Other studies have dealt with the behavior of smoke particles in a smoldering phase (a particulate phase which is known to be highly dominated by the organic matter) [*Patterson and McMahon*, 1984; *Tangren*, 1982; D. Campbell et al., A method for optical characterization of aerosols produced by biomass combustion, submitted to *Environmental Science and Technology*, 1995]. The mean scattering cross-section that these authors have measured for the smoke particles ranges from 2.6 to 3.6 m^2/g. Taking the above studies into consideration, we selected a mean specific scattering cross section of 4 m^2/g for organic matter at 0.55 µm, for low relative humidity conditions. Since we could not find any experimental data on the wavelength dependence of this parameter, we used that determined for BC. To take into account the hydrophilic behavior of the organic matter reported by previous authors [*Ducret and Cachier*, 1992; *Novakov and Penner*, 1993], we assumed that the particle coefficients would be affected by an increase of the relative humidity from 30% to 85%, similar to that assumed for sulfate aerosols [*Kiehl and Briegleb*, 1993]. This assumption increases the scattering cross section for OM to 6.8 m^2/g at a relative humidity of 80%.

Plates 3a and 3b show the calculated single scattering albedo for an average relative humidity of 80%, assuming the column abundances of OC, BC, and sulfate aerosol calculated by the model in January and July. The global patterns of the simulated single scattering albedos are very different in January and July.

In the northern hemisphere, much of the variation is due to the seasonal variability of the different components of the aerosol. This model, in keeping with observations in North America, has a strong seasonal variation in sulfate abundance with less production in the winter hemisphere [*Penner et al.*, 1994]. On the other hand, the simulated concentrations of carbonaceous particles, in agreement with observed northern hemisphere concentrations [*Cachier*, 1995], have similar abundances in summer and winter. Hence much lower albedos are obtained in the northern hemisphere winter, where sulfate aerosols are significantly decreased over absorbing BC particles.

The southern hemisphere and tropics are mainly polluted by biomass burning sources. Here, carbonaceous particles dominate the sulfate aerosol, and the variability of the single scattering albedo is governed by the fire season. The global distribution of ω_0 is therefore mainly determined by the global distribution of BC particles and OM. As shown in Plates 3a and 3b, the single scattering albedo is lower in January north of the equator and is lower in July, south of the equator.

Because the measured aerosol single scattering albedo is sensitive to the presence of BC, a comparison of our model-generated albedo with data represents a test of the model's predicted concentrations. Of course, if the measured albedos represent an aerosol with scattering components other than OC, BC, and sulfate (together with its chemically bound ammonium) that contribute to the measured single scattering albedos, we would expect the model-predicted values to be lower than those measured. Table 8 compares the model-predicted and measured single scattering albedos at a number of rural and remote locations. Because measurements of single scattering albedo are normally obtained under dry conditions, we used the dry scattering cross sections reported above, namely, 5 and 4 m^2/g for sulfate aerosol and organic matter, respectively. The simulated and observed single scattering albedos are in reasonable agreement, though the model appears to be somewhat low in some locations (e.g. the Arctic, Spitsbergen, the Equator, and Australia). According to this test, the model captures most of the important scattering and absorbing species at most locales.

According to *Hansen et al.* [1980] and *Bergström et al.* [1982], aerosols with single scattering albedo less than 0.85 mainly warm the planet, while those with ω_0 greater than 0.85 cool the planet. Plates 3a and 3b demonstrate that the aerosols represented in the model would mainly have a cooling effect, except in the most polluted regions.

5. Conclusion

This study focused on the use of the Grantour model to calculate the transport of both BC particles and OM in the troposphere. We developed source inventories for these aerosols for biomass burning in savanna, forest, agricultural, and domestic fires. The fossil fuel sources of BC were estimated from previously developed inventories. Natural anthropogenic fires of the temperate and boreal regions which may represent as much as 10% of the total biomass burning have not yet been included. This omission may explain some of the low concentrations predicted during the summer season. Aircraft may represent an important source in the upper troposphere but were not included in our study. We made a simple estimate of the organic matter inventory from fossil fuel and urban related sources. For that purpose, we have assumed a constant for the ratio of BC to OM and used the BC inventory previously described. It is important to improve this description in order to account for geographical

Table 7. Mean Optical Cross Sections for Black Carbon and Organic Matter in the UV, Visible, and IR Wavelengths

	Wavelength, in µm		
Specific Cross Section, m^2/g	0.3	0.55	1.06
BC absorption cross section	10	7	3
BC scattering cross section	3.5	1.95	1
OM scattering cross section	7	4	2.1
Sulfate scattering cross section	9.9	5	0.9

Table 8. Comparison of the Calculated and Measured Single Scattering Albedo Values for a Subset of Locations

		Single Scattering Albedo		
Location	Time Period	Observed	Simulated	References
71.2N, 156.3W (Barrow)	Annual	0.90-0.95	0.91-0.95	*Bodhaine* [1995]
89S, 102W (South Pole)	Annual	0.95	0.97	*Bodhaine* [1995]
82.5S, 62.5W (Arctic)	Summer	0.975	0.94	*Heintzenberg* [1982]
	Winter	0.95	0.90	*Heintzenberg* [1982]
79N, 12W (Spitsbergen)	Annual	0.93-0.97	0.90-0.92	*Heintzenberg and Leck* [1994]
25S, 135E (Australia)	Annual	1	0.96	*Clarke* [1989]
19.3N, 155.4W (Mauna Loa)	Annual	0.93-0.96	0.93	*Bodhaine* [1995]
0.1S, 49W (Amazonia)	Annual	0.93	0.92	*Kaufman et al.* [1992]
2S, 77.3W (Equator)	Annual	0.99	0.97	*Clarke* [1989]
59.2N, 18E (Stockholm)	Annual	0.89	0.87	*Heintzenberg* [1982]
38.3N, 80W (Allegheny Mt.)	Annual	0.87	0.91	*Japar et al.* [1986]
38N, 78W (Shenandoah)	Summer	0.95	0.91-0.97	*Ferman et al.* [1981]
56N, 160E (Kamchatka)	Annual	0.92	0.90-0.92	*Clarke* [1989]
37.1N, 108.3W (Mesa Verde)	Annual	0.94	0.94	*Waggoner et al.* [1981]
41.4N, 42.5E (Abastumani)	Annual	0.86-0.92	0.82-0.89	*Waggoner et al.* [1981]

Ranges refer to the minimum and maximum observed values.

variability in the BC/OM ratio. A simple scheme was used to covert terpenes into natural organic matter. An important improvement would introduce more realism into the model by including, for example, photochemical conversion of gaseous emissions to particular forms. Additionally, other natural sources such as the primary particle emissions from vegetation should be better quantified so that they might be included.

The model formulation has been tested by comparison of the model-predicted surface concentrations and concentration in precipitation with observed data. There is generally good agreement between the model and observations measured in rural and remote sites, except for a few critical areas which point out the need for further improvement. Some of these are linked to source improvements (see above), others to the model formulation and transport fields. We demonstrated that the predicted results are highly dependent on the choice of the scavenging ratio and injection height, especially in remote areas, where for example, the simulated surface concentrations may be changed by a factor of 2 for a change in scavenging coefficient of only 15%. This sensitivity implies that improved treatments of aerosol scavenging, based on more realistic physical treatments, such as the inclusion of size-dependent scavenging effects, may yield important improvements in the model formulation. It further implies that measurements of BC and OM at remote locations can provide sensitive tests for the model.

During this study, we also constructed global maps of the aerosol single scattering albedo. These maps illustrate the fact that the global impact of the carbonaceous aerosol in combination with sulfate is likely to be a cooling effect [*Penner et al.*, 1996]. In future work, the contribution of dust particles will also be considered.

Acknowledgments. This work was performed under the auspices of the U.S. Department of Energy under Contract W-7405-Eng-48. Support from the NASA Aerosol Program and the DOE Quantitative Links Program is gratefully acknowledged.

References

Anderson, T.L., and O. Boucher, The sensitivity of direct climate forcing by sulfate aerosols to aerosol size and chemistry, paper presented at the Fourth International Aerosol Conference, American Association for Aerosol Research, Los Angeles, Calif., Aug. 29 to Sept. 2, 1994.

Andreae, M.O., Soot carbon and excess potassium: Long range transport of combustion-derived aerosols, *Science, 220,* 1148–1151, 1983.

Andreae, M.O., Biomass burning: Its history, use and distribution and its impact on environmental quality and global climate, in *Global Biomass Burning*, edited by J. S. Levine, pp. 1–21, MIT Press, Cambridge, Mass., 1991.

Andreae, M.O., T.W. Andreae, R.J. Ferek, and H. Raemdonck, Long-range transport of soot carbon in the marine atmosphere, *Sci. Total Environ., 36,* 73–80, 1984.

Andreae, M.O., et al., Airborne studies of aerosol emissions from savanna fires in southern Africa (abstract), *EOS Trans. AGU, 74*(43), Fall Meet. Suppl., 128, 1993.

Andreae, M.O., B.E. Anderson, D.R. Blacke, J.D. Bradshaw, J.E. Collins, G.L. Gregory, G.W. Sachse, and M.C. Shipham, Influence of plumes from biomass burning on atmospheric chemistry over the equatorial and tropical south Atlantic during CITE 3, *J. Geophys. Res., 99,* 12,793–12,808, 1994.

Artaxo, P., F. Gerab, M.A. Yamasoe, J.V. Martins, and A. Setzer, Trace elements and black carbon in aerosol particles in the Amazon basin, paper presented at the Fifth International Conference on Carbonaceous Aerosols, U.S. Dept. of Energy, Berkeley, Calif., Aug. 23–26, 1994.

Barnard, G., and L. Kristoferson, Agricultural residues as fuel in the third world, *Tech. Rep. 4*, 178 pp., Earthscan, International Institute for Environment and Development, London, 1985.

Benkovitz, C.M., C.M. Berkowitz, R.C. Easter, S. Nemesure, R. Wagener, and S.E Schwartz, Sulfate over the North Atlantic and adjacent continental regions: Evaluation for October and November 1986 using a three-dimensional model driven by observation-derived meteorology, *J. Geophys. Res., 99,* 20,725–20,756, 1994.

Bergström, R.W., T.P. Ackerman and L.W. Richards, The optical properties of particulate elemental carbon, in *Particulate Carbon: Atmospheric Life Cycle*, edited by G.T. Wolff and R.L. Klimisch , pp. 43–48, Plenum, New York, 1982.

Blake, D., and K. Kato, Latitudinal distribution of black carbon soot in the upper troposphere and lower stratosphere, *J. Geophys. Res., 100,* 7195–7202, 1995.

Bodhaine, B.A., Aerosol absorption measurements at Barrow, Mauna Loa, and the south pole, *J. Geophys. Res., 100,* 8967–8975, 1995.

Brémond, M.P., H. Cachier, and P. Buat-Ménard, Particulate carbon in the Paris region atmosphere, *Environ. Tech. Lett., 10,* 339–346, 1989.

Brown, S., A.J.R. Gillespie, and A.E. Lugo, Biomass estimation methods for tropical forests with applications to forest inventory data, *Forest Sci., 35,* 881–902, 1989.

Bryson, R.A., and F.K. Hare, *Climates of North America, World Survey of Climatology*, vol. 11, 420 pp., Elsevier, New York, 1974.

Butcher, S.S., and M.J. Ellenbecker, Particulate emission factors for small wood and coal stoves, *J. Air Pollut. Contr. Assoc., 32,* 380–384, 1982.

Butcher, S.S., and E.M. Sorenson, A study of wood stove particulate emissions, *J. Air Pollut. Contr. Assoc.*, 29, 724–728, 1979.

Butcher, S.S., U. Rao, K.R. Smith, J. Osborn, P. Azuma, and H. Fields, Emission factors and efficiencies for small-scale open biomass combustion: Towards standard measurement techniques, paper presented at the Annual Meeting, Am. Chem. Soc., Div. of Fuel Chem., Philadelphia, Pa., Aug. 26–31, 1984.

Cachier, H., Biomass burning sources, in *Encyclopedia of the Earth System Science*, edited by W.A. Nierenberg, vol. 1, pp. 377–385, Academic, San Diego, Calif.,1992.

Cachier, H., Combustion carbonaceous aerosols in the atmosphere: Implications for ice-core studies, in *Ice Core Studies of Biogeochemical Cycles, Nato ASI Ser.*, edited by R. Delmas, vol. 30, pp. 347–360, Springer-Verlag, New York, 1995.

Cachier, H., and J. Ducret, Influence of biomass burning on equatorial African rains, *Nature, 352*, 228–230, 1991.

Cachier, H., M.P. Brémond, and P. Buat-Ménard Organic and black carbon aerosols over marine regions of the northern hemisphere, in Proceedings of the International Conference on Global Atmospheric Chemistry, edited by L. Newman and C.S. Kiang, 241–261, Brookhaven National Laboratory Press, Brookhaven, NY, 1990.

Cachier, H., P. Buat-Ménard, M. Fontugne, and R. Chesselet, Long-range transport of continentally-derived particulate carbon in the marine atmosphere: Evidence from stable carbon isotope studies, *Tellus, 38B*, 161–177, 1986.

Cachier, H., C. Liousse, A. Cachier, B. Ardouin, G. Polian, V. Kazan, and A.D.A. Hansen, Black carbon aerosols at the remote site of Amsterdam Island, paper presented at the Fifth International Conference on Carbonaceous Aerosols, U.S. Dept. of Energy, Berkeley, Calif., Aug. 23–26, 1994.

Cachier, H., C. Liousse, P. Buat-Ménard, and A. Gaudichet, Particulate content of savanna fire emissions, *J. Atmos. Chem.*, *22*, 123–148, 1995.

Cadle, S.H. and J.M. Dasch, Wintertime concentration and sinks of atmospheric particulate carbon at a rural location in northern Michigan, *Atmos. Environ.*, *22*, 1373–1381, 1988.

Cahoon, D.R., B.J. Stocks, J.S. Levine, W.R. Cofer III, and K.P. O'Neil, Seasonal distribution of African savanna fires, *Nature*, *359*, 812–815, 1992.

Cahill, T.A., R.A. Eldred, L.K. Wilkinson, B.P. Derley, and W.C. Malm, Spatial and temporal trends of fine particles at remote U.S. sites, in *Proceedings of the 83rd Annual Meeting and Exhibition of the Air and Waste Management Association*, pp. 24–29, Air and Waste Management Assn. Press, Pittsburgh, Pa., 1990.

Carroll, J.J., G.E. Miller, J.F. Thompson, and E.F. Darley, The dependence of open field burning emissions and plume concentrations on meteorology, field conditions and ignition technique, *Atmos. Environ.*, *11*, 1037–1050, 1977.

Charlson, R.J., J. Langner, H. Rodhe, C.B. Leovy, and S.G. Warren, Perturbation of the northern hemisphere radiative balance by backscattering from anthropogenic sulfate aerosols, *Tellus*, *43AB*, 152–163, 1991.

Chesselet, R., M. Fontugne, P. Buat-Menard, U. Ezat, and C.E. Lambert, The origin of particulate organic carbon in the marine atmosphere as indicated by its stable carbon isotopic composition, *Geophys. Res. Lett.*, *8*, 345–348, 1981.

Chuang, C.C., and J.E. Penner, Effects of aerosol sulfate on cloud drop nucleation and optical properties, *Tellus*, *47B*, 566–577, 1995.

Chuang, C.C., J.E. Penner, K.E. Taylor, and J.J. Walton, Climate effects of anthropogenic sulfate: Simulations from a coupled chemistry/climate model, in *Proceedings of the Conference on Atmospheric Chemistry*, pp. 170–174, Am. Meteorol. Soc., Boston, Mass., 1994.

Chylek, P., V. Srivastava, L. Cahenzli, R.G. Pinnick, R.L. Dod, T. Novakov, T.L. Cook, and B.D. Hinds, Aerosol and graphitic carbon content of snow, *J. Geophys. Res.*, *92*, 9801–9809, 1987.

Clarke, A.D., Aerosol light absorption by soot in remote environments, *Aerosol Sci. Technol.*, *10*, 161–171, 1989.

Clarke, A.D., and K.J. Noone, Soot in the Arctic snowpack: A cause for perturbations in radiative transfer, *Atmos. Environ.*, *19*, 2045–2053, 1985.

Cooke, W.F., and J.J.N. Wilson, A global black carbon aerosol model, *J. Geophys. Res.*, this issue.

Cooper, J., Environmental impact of residential wood combustion emissions and its implications, *J. Air Pollut. Contr. Assoc.*, *30*, 855–861, 1980.

Countess, R.J., S.H. Cadle, P.J. Groblicki, and G.T. Wolff, Chemical analysis of size-segregated samples of Denver's ambient particulate, *J. Air Pollut. Contr. Assoc.*, *31*, 247–252, 1981.

Crutzen, P.J., and M.O. Andreae, Biomass burning in the tropics: Impact on atmospheric chemical and biogeochemical cycles, *Science*, *250*, 1669–1678, 1990.

D'Almeida, G.A., P. Koepke, and E.P. Shettle, *Atmospheric Aerosols: Global Climatology and Radiative Characteristics*, 561 pp., A. Deepak, Hampton, Va., 1991.

Darley, E.F., F.R. Burleson, E.H. Mateer, J.T. Middleton, and V.P. Osterli, Contribution of burning of agricultural wastes to photochemical air pollution, *J. Air Pollut. Contr. Assoc.*, *16*, 685–690, 1966.

Dasch, J.M., Particulate and gaseous emissions from wood-burning fireplaces, *Environ. Sci. Technol.*, *16*, 639–645, 1982.

De Angelis, D.G., D.S. Ruffin, J.A. Peters, and R.B. Reznik, Source assessment: Residential combustion of wood, *Rep. EPA 60012-80-042b*, U.S. Environmental Protection Agency, Washington, D.C., 1980.

Delmas, R., P. Loudjani, and A. Podaire, Biomass burning in Africa: An assessment of annually burned biomass, in *Global Biomass Burning*, edited by J.S. Levine, pp. 126–132, MIT Press, Cambridge, Mass., 1991.

Dignon, J. and J.E. Penner, Biomass burning: A source of nitrogen oxides in the atmosphere, in *Global Biomass Burning*, edited by J.S. Levine, pp. 370–375, MIT press, Cambridge, MA, 1991.

Dobbins, R.A., G.W. Mulholland, and N.P. Bryner, Comparison of a fractal smoke optics model with light extinction measurements, *Atmos. Environ.*, *28*, 889–897, 1994.

Duce, R.A., Speculations on the budget of particulate and vapor phase non-methane organic carbon in the global troposphere, *Pure Appl. Geophys.*, *116*, 245–273, 1978.

Ducret, J., and H. Cachier, Particulate carbon in rain at various temperate and tropical locations, *J. Atmos. Chem.*, *15*, 55–67, 1992.

Dzubay, T.G., R.K. Stevens, and P.L. Haagenson, Composition and origins of aerosol at a forested mountain in Soviet Georgia, *Environ. Sci. Technol.*, *18*, 873–883, 1984.

Fenn, R.W., and H. Oser, Scattering properties of concentric soot-water spheres for visible and infrared light, *Appl. Opt.*, *4*, 1504–1509, 1965.

Ferman, M.A., G.T. Wolff and N.A. Kelly, The nature and sources of haze in the Shenandoah Valley/Blue Ridge Mountains area, *J. Air Pollut. Control. Assoc.*, *31*, 1074–1082, 1981.

Fischer, R.A., Wheat, in *Symposium on Potential Productivity of Field Crops Under Different Environments*, 129–154, Int. Rice Res. Inst., Manila, Philippines, 1983.

Fisher, K.S., and A.F.E. Palmer, Maize, in *Symposium on Potential Productivity of Field Crops on Different Environments*, 155–180, Int. Rice Res. Inst., Manila, Philippines, 1983.

Food and Agriculture Organization, *FAO Production Yearbook, 45*, 265 pp., Rome, 1991.

Gaffney, J.S., R. L. Tanner, and M. Phillips, Separating carbonaceous aerosol source terms using thermal evolution, carbon isotopic measurements, and C/N/S determinations, *Sci. Total Environ.*, *36*, 53–60, 1984.

Gerstle, R.W., and D.A. Kemnitz, Atmospheric emissions from open burning, *J. Air Pollut. Contr. Assoc.*, *17*, 324–327, 1967.

Gray, H.A., G.R. Cass, J.J. Huntzicker, E.K. Heyerdahl, and J.A. Rau, Elemental and organic carbon particle concentrations: A long-term perspective, *Sci. Total Environ.*, *36*, 17–25, 1984.

Guenther, A., et al., A global model of natural volatile organic compound emissions, *J. Geophys. Res.*, *100*, 8873–8892, 1995.

Hammond, A.L., Editor-in-Chief, *World Resources 1992-1993*, 385 pp., Oxford Univ. Press, New York, 1992.

Hansen, A.D.A., B.A. Bodhaine, E.G. Dutton, and R.C. Schnell, Aerosol black carbon measurement at the South Pole: Initial results, 1986-1987, *Geophys. Res. Lett.*, *15*, 1193–1196, 1988.

Hansen, J., D. Johnson, A. Lacis, S. Lebedeff, P. Lee, D. Rind, and G. Russel, Climate impact of increasing atmospheric carbon dioxide, *Science*, *213*, 957–966, 1980.

Hao, W.M. and M.-H. Liu, Spatial and temporal distribution of tropical biomass burning, *Global Biogeochem. Cycles*, *8*, 495–503, 1994.

Hao, W.M., M.H. Liu, and P.J. Crutzen, Estimates of annual and regional releases of CO_2 and other trace gases to the atmosphere from fires in the tropics, based on the FAO statistics for the period 1975-1980, in *Fire in the Tropical Biota*, edited by J.C. Goldammer, pp. 440–462, Springer-Verlag, Berlin, 1990.

Hatakeyama, S., K. Izumi, T. Fukuyama, H. Akimoto, and N. Washida, Reactions of OH with α-pinene and β-pinene in air: Estimate of global CO production from the atmospheric oxidation of terpenes, *J. Geophys Res.*, *96*, 947–958, 1991.

Heintzenberg, J., Measurement of light absorption and elemental carbon in atmospheric aerosol samples from remote locations, in *Particulate Carbon: Atmospheric Life Cycle*, edited by G.T. Wolff and R.L. Klimisch, pp. 371–377, Plenum, New York, 1982.

Heintzenberg, J., and E.K. Bigg, Tropospheric transport of trace substances in the southern hemisphere, *Tellus*, *42B*, 355–363, 1990.

Heintzenberg, J., and C. Leck, Seasonal variation of the atmospheric aerosol near the top of the marine boundary layer over Spitsbergen related to the Arctic sulfur cycle, *Tellus*, *46B*, 52–67, 1994.

Héry, J.L., Caractérisation des émissions particulaires par combustion de biomasse végétale: exemple d'une savane sèche d'Afrique du Sud. Fabrication artisanale de charbon de bois, 26 pp,. Master, Univ. Paris VII, 1993.

Hidy, G.M., P.K. Mueller, H.H. Wang, J. Karney, S. Twiss, M. Imada, and A. Alcocer, Observations of aerosols over southern California coastal waters, *J. Appl. Meteorol.*, *13*, 96–107, 1974.

Hoffman, E.J., and R.A. Duce, Organic carbon in marine atmospheric particulate matter: Concentration and particle size distribution, *Geophys. Res. Lett.*, *4*, 449–452, 1977.

Holben, B. N., Y.J. Kaufman, A.W. Setzer, D.D. Tanré, and D.E. Ward, Optical properties of aerosol emissions from biomass burning in the tropics, BASE-A, in *Global Biomass Burning*, edited by J. S. Levine, pp. 403–411, MIT Press, Cambridge, Mass., 1991.

Hopper, J. F., L.A. Barrie, N.B. Trivett, and D.J. Worthy, Continuous measurements of black carbon and related species at Alert, Canada, paper presented to the Fourth International Conference on Carbonaceous Aerosols, Austrian Federal Ministries of Environment, and Science and Technology, Vienna, April 3–5, 1991.

Irvine, J.E., Sugarcane, in *Symposium on Potential Productivity of Field Crops on Different Environments*, 361–381, Int. Rice Res. Inst., Manila, Philippines, 1983.

Japar, S.M., A.C. Szkarlat, and W.R. Pierson, The determination of the optical properties of airborne particle emissions from diesel vehicles, *Sci. Total Environ.*, *36*, 121–130, 1984.

Japar, S.M., W.W. Brachaczek, R.A. Gorse Jr., J.M. Norbeck, and W.R. Pierson, The contribution of elemental carbon to the optical properties of rural atmospheric aerosols, *Atmos. Environ.*, *20*, 1281–1289, 1986.

Jenkins, B.M., S.Q. Turn, R.B. Williams, D.P.Y. Chang, O.G. Raabe, J. Paskind, and S. Teague, Quantitative assessment of gaseous and condensed phase emissions from open burning of biomass in a combustion wind tunnel, in *Global Biomass Burning*, edited by J. S. Levine , 305–317, MIT Press, Cambridge, Mass., 1991.

Jenkins, B.M., I.M. Kennedy, S.Q. Turn, R.B. Williams, S.G. Hall, S.V. Teague, D.P.Y. Chang, and O.G. Raabe, Wind tunnel modeling of atmospheric emissions from agricultural burning: Influence of operating configuration on flame structure and particle emission factor for a spreading-type fire, *Environ. Sci. Technol.*, *27*, 1763–1775, 1993.

Jennings, S.G., and C.D. O'Dowd, Volatility of aerosol at Mace Head on the West Coast of Ireland, *J. Geophys. Res.*, *95*, 13,937-13,948, 1990

Jennings, S.G., and R.G. Pinnick, Relationship between visible extinction, absorption and mass concentration of carbonaceous smokes, *Atmos. Environ.*, *14*, 1123–1129, 1980.

Jennings, S.G., F.M. McGovern, and W.F. Cooke, Carbon mass concentration measurements at Mace Head, on the West Coast of Ireland, *Atmos. Environ.*, *27A*, 1229–1239, 1993.

Kaufman, T.J., A. Setzer, D. Ward, D. Tanré, B.N. Holben, P. Menzel, M.C. Pereira, and R. Ramussen, Biomass burning airborne and space borne experiment in the Amazonas (Base-A), *J. Geophys. Res.*, *97*, 14,581–14,599, 1992.

Ketsediris, G., J. Hahn, R. Jaenicke and C. Junge, The organic constituents of atmospheric particulate matter, *Atmos Environ.*, *10*, 603-610, 1976.

Kiehl, J.T., and B.P. Briegleb, The relative roles of sulfate aerosols and greenhouse gases in climate forcing, *Science*, *260*, 311–314, 1993.

Lacaux, J.P., J.M. Brustet, R. Delmas, J.C. Menaut, L. Abbadie , B. Bonsang, H. Cachier, J.G.R. Baudet, M.O. Andreae and G. Helas, Biomass burning in the tropical savannas of Ivory Coast: An overview of the field experiment Fire of Savannas (FOS/DECAFE '91), *J. Atmos. Chem.*, *22*, 195–216, 1995.

Lambert, G., G. Polian, J. Sanak, B. Ardouin, A. Buisson, A. Jegou and J.C. Le Roulley, Cycle du radon et de ses descendants: Application a l'etude des echanges troposphere-stratosphere, *Ann. Geophys.*, *4*, 497–531, 1982.

Langner, J., and H. Rodhe, A global three-dimensional model of the tropospheric sulfur cycle, *J. Atmos. Chem.*, *13*, 225–263, 1991.

Langner, J., H. Rodhe, P.J. Crutzen, and P. Zimmermann, Anthropogenic influence on the distribution of tropospheric sulphate aerosol, *Nature*, *359*, 712–716, 1992.

Le Canut, P., M.O. Andreae, G.W. Harris, F.G. Wienhold, and T. Zenker, Airborne studies of emissions from savanna fires in southern Africa, 1, Aerosol emissions measured with a laser-optical particle counter, *J. Geophys. Res.*, in press, 1996.

Levine, J.S., Global biomass burning: Atmospheric, climatic and biospheric implications, *Eos Trans. AGU*, *71*, 37, 1990.

Liousse, C., H. Cachier, and S.G. Jennings, Optical and thermal measurements of black carbon aerosol content in different environments: Variation of the specific attenuation cross-section, sigma (σ), *Atmos. Environ.*, *27*, 1203–1211, 1993.

Liousse, C., J.R.A. Franca, H. Cachier, and F. Dulac, Monitoring of carbonaceous aerosols at Lamto, Ivory Coast and comparison with fire pixel numbers retrieved from AVHRR satellite data, paper presented to the Fifth International Conference on Carbonaceous Aerosols, U.S. Department of Energy, Berkeley, Calif., Aug. 23–26, 1994.

Liousse, C., C. Devaux, F. Dulac and H. Cachier, Aging of savanna biomass burning aerosols: Consequences on their optical properties, *J. Atmos. Chem.*, *22*, 1–17, 1995.

Luecken, D.J., C.M. Berkowitz, and R.C. Easter, Use of a three-dimensional cloud-chemistry model to study the trans-Atlantic transport of soluble sulfur species, *J. Geophys. Res.*, *96*, 22,477–22,490, 1991.

Mahtab, F.U., and M.N. Islam, Biomass availability from field crops, paper presented for Bangladesh Energy Planning Project Rural Energy Course, Government of Bangladesh, Dhaka, 1984.

Malm, W.C., J.F. Sisler, D. Huffman, R.A. Eldred and T.A. Cahill, Spatial and seasonal trends in particle concentration and optical extinction in the United States, *J. Geophys. Res.*, *99*, 1347–1370, 1994.

Meland, B.R. and R.W. Boubel, A study of field burning under varying environmental conditions, *J. Air Pollut. Contr. Assoc.*, *16*, 481–484, 1966.

Menaut, J.C., L. Abbadie, F. Lavenu, P. Loudjani and A. Podaire, Biomass burning in west African savannas, in *Global Biomass Burning*, edited by J. S. Levine, pp. 133–142, MIT Press, Cambridge, Mass., 1991.

Middleton, J.T., and E.F. Darley, Control of air pollution affecting or caused by agriculture, in *Pollution: Engineering and Scientific Solutions*, edited by E.S. Barrekette, pp. 148–157, Plenum, New York, 1973.

Muhlbaier, J.L., and R.L. Williams, Fireplaces, furnaces and vehicles as emissions sources of particulate carbon, in *Particulate Carbon: Atmospheric Life Cycle*, edited by G.T. Wolff and R.L. Klimisch , pp. 185–198, Plenum, New York, 1982.

Mukai, H., Y. Ambe, K. Shibata, T. Muku, K. Takeshita, T. Fukuma, J. Takahashi, and S. Mizota, Long-term variation of chemical composition of atmospheric aerosols on the Oki Islands in the Sea of Japan, *Atmos. Environ.*, *24*, 1379–1390, 1990.

Novakov, T. Soot in the atmosphere, in *Particulate Carbon: Atmospheric Life Cycle*, edited by G.T. Wolff and R.L. Klimisch , pp. 19–37, Plenum, New York, 1982.

Novakov, T., and J.E. Penner, Large contribution of organic aerosols to cloud-condensation-nuclei concentrations, *Nature*, *365*, 823–826, 1993.

Ogren, J.A. and R.J. Charlson, Wet deposition of elemental carbon and sulfate in Sweden, *Tellus*, *36B*, 262–271, 1984.

Ogren, J.A., P.J. Groblicki and R.J. Charlson, Measurement of the removal rate of elemental carbon from the atmosphere, *Sci. Total. Environ.*, *36*, 329–338, 1984.

Openshaw, K., Wood fuels in the developing world, *New Sci.*, *61*, 271–272, 1974.

Pandis, S.N., S.E. Paulson, J.H. Seinfeld, and R.C. Flagan, Aerosol formation in the photooxidation of isoprene and β-pinene, *Atmos. Environ.*, *25A*, 997–1008, 1991.

Parungo, F., B. Kopcewicz, C. Nagamoto, R. Schnell, P. Sheridan, C. Zhu, and J. Harris, Aerosol particles in the Kuwait oil fire plumes: Their morphology, size distribution, chemical composition, transport, and potential effect on climate, *J. Geophys. Res.*, *97*, 15,867–15,882, 1992.

Parungo, F., C. Nagamoto, M.Y. Zhou, A.D.A. Hansen and J. Harris, Aeolian transport of aerosol black carbon from China to the ocean, *Atmos. Environ.*, *28*, 3251–3260, 1994.

Patterson, E.M., and C.K. McMahon, Absorption characteristics of forest fire particulate matter. *Atmos. Environ. 18*, 2541–2551, 1984.

Penner, J.E., Carbonaceous aerosols influencing atmospheric radiation: Black and organic carbon, in *Aerosol Forcing of Climate*, edited by R.J. Charlson and J. Heintzenberg, pp. 91–108, John Wiley, New York, 1995.

Penner, J.E., C.S. Atherton, J. Dignon, S.G. Ghan, J.J. Walton, and S. Hameed, Tropospheric nitrogen: A three-dimensional study of

sources, distributions, and deposition, *J. Geophys. Res.*, *96*, 959–990, 1991b.

Penner, J.E., S.J. Ghan and J.J. Walton, The role of biomass burning in the budget and cycle of carbonaceous soot aerosols and their climate impact, in *Global Biomass Burning*, edited by J. S. Levine, pp. 387–393, MIT Press, Cambridge, Mass., 1991a.

Penner, J.E., R.E. Dickinson, and C.A. O'Neill, Effects of Aerosol from biomass burning on the global radiation budget, *Science*, *256*, 1432–1434, 1992.

Penner, J.E., H. Eddleman, and T. Novakov, Towards the development of a global inventory for black carbon emissions, *Atmos. Environ.*, *27A*, 1277–1295, 1993.

Penner, J.E., C.A. Atherton, and T.E. Graedel, Global emissions and models of photochemically active compounds, in *Global Atmospheric-Biospheric Chemistry*, edited by R. Prinn, pp. 223–248, Plenum, New York, 1994.

Penner, J.E., T. Wigley, P. Jaumann, B. Santer, and K. Taylor, Anthropogenic sulfate aerosols and climate change: A method for calibrating forcing, in *Communicating About Climate: The Story of the Model Evaluation Consortium for Climate Assessment*, edited by W. Howe and A. Henderson-Sellers, Gordon and Breach, Roseville East, Australia, in press, 1996.

Pham, M., J.F. Muller, G. Brasseur, C. Granier, and G. Megie, A three dimensional study of the tropospheric sulfur cycle, *J. Geophys. Res.*, *100*, 26,061–26,092, 1995.

Pierson, W.R., and P.A. Russell, Aerosol carbon in the Denver area in November 1973, *Atmos. Environ.*, *13*, 1623–1628, 1979.

Piispanen, W., W.M. Cooke, and J.M. Allen, A sampling method for the characterization of carbonaceous emissions from wood-fueled residential heating appliances, *Sci. Total Environ.*, *36*, 159–168, 1984.

Pueschel, R.F., J.M. Livingston, G.V. Ferry, and T.E. De Felice, Aerosol abundances and optical characteristics in the Pacific basin free troposphere, *Atmos. Environ.*, *28*, 951–960, 1994.

Radke, L.F., D.A. Hegg, J.H. Lyons, C.A. Brock, P.V. Hobbs, R.E. Weiss, and R. Rasmussen, Airborne measurements on smokes from biomass burning, in *Aerosols and Climate*, edited by P. Hobbs and P. Mc Cormick, pp. 411–422, A. Deepak, Hampton, 1988.

Riehl, H. (ed.), *Climate and Weather in the Tropics*, 61 pp., Academic, San Diego, Calif., 1979.

Robertson, G.P., and T. Rosswall, Nitrogen in West Africa: The regional cycle, *Ecol. Monogr.*, *56*, 43–72, 1986.

Robinson, J.M., On uncertainty in the computation of global emissions from biomass burning, *Clim. Change*, *14*, 243–262, 1989.

Roessler, D.M., and F.R. Faxvog, Optoacoustic measurement of optical absorption in acetylene smoke, *J. Opt. Soc. Am.*, *69*, 1699–1704, 1979.

Rosen, H., A.D.A. Hansen, R.L. Dod, and T. Novakov, Soot in urban atmospheres: Determination by an optical absorption technique, *Science*, *208*, 741–744, 1980.

Seiler, W., and P.J. Crutzen, Estimates of gross and net fluxes of carbon between the biosphere and the atmosphere from biomass burning, *Clim. Change*, *2*, 207–247, 1980.

Sexton, K., J.D. Spengler, R.D. Treitman, and W.A. Turner, Winter air quality in a wood burning community: A case study in Waterbury, Vermont, *Atmos. Environ.*, *18*, 1357–1370, 1984.

Sloane, C.S., Optical properties of aerosols--Comparison of measurements with model calculations, *Atmos. Environ.*, *17*, 409–416, 1983.

Sloane, C. S., Optical properties of aerosols of mixed composition, *Atmos. Environ.*, *18*, 871–878, 1984.

Smith K.R., A.L. Aggarwal, and R.M. Dave, Air pollution and rural biomass fuels in developing countries: A pilot village study in India and implications for research and policy, *Atmos. Environ.*, *17*, 2343–2362, 1983.

Strehler, A., and W. Stutzle, Biomass residues, in *Biomass Renewable Energy*, edited by D.O. Hall and R.P. Overend, pp. 75–102, John Wiley, New York, 1987.

Tangren, C.D., Scattering coefficient and particulate matter concentration in forest fire smoke, *J. Air Pollut. Contr. Assoc.*, *32*, 729–732, 1982.

Taylor, K.E., and J.E. Penner, Response of the climate system to atmospheric aerosols and greenhouse gases, *Nature*, *369*, 734–737, 1994.

Turn, S.Q., B.M. Jenkins, J.C. Chow, L.C. Pritchett, D. Campbell, and T. Cahill, Elemental characterization of particulate matter emitted from biomass burning: Wind tunnel derived source profiles for straw and wood fuels, (abstract), *Eos Trans. AGU*, *74*(43), Fall Meet. Suppl., 104, 1993.

Twitty , J.T., and J.A. Weinman, Radiative properties of carbonaceous aerosols, *J. Appl. Meteorol.*, *10*, 725–731, 1971.

Valaoras, G., J.J. Huntzicker and W.H. White, On the contribution of motor vehicles to the Athenian "nephos": An application of factor signature, *Atmos. Environ.*, *22*, 965–971, 1988.

Waggoner, A.P., R.E. Weiss, N.C. Ahlquist, D.S. Covert, S. Will and R.J. Charlson, Optical characteristics of atmospheric aerosols, *Atmos. Environ.*, *15*, 1891–1909, 1981.

Walton, J.J., M.C. MacCracken, and S.J. Ghan, A global-scale Lagrangian trace species model of transport, transformation, and removal process, *J. Geophys. Res.*, *93*, 8339–8354, 1988.

Ward, D.E., A.W. Setzer, Y.J. Kaufman, and R.A. Rasmussen, Characteristics of smoke emissions from biomass fires of the Amazon region-Base-A experiment, in *Global Biomass Burning*, edited by J. S. Levine, pp. 394–402, MIT Press, Cambridge, Mass., 1991.

Warren, S.G., and A.D. Clarke, Soot in the atmosphere and snow surface of Antarctica, *J. Geophys. Res.*, *95*, 1811–1816, 1990.

Williamson, G.S., and D.L. Williamson, Circulation statistics from seasonal and perpetual January and July simulations with the NCAR Community Climate Model (CCM1): R15, *NCAR Tech. Note, NCAR/TN-302+STR*, 199 pp., (Available as *NTIS PF88-192620/AS*, from Natl. Tech. Inf. Serv., Springfield, Va.), Natl. Cent. for Atmos. Res., Boulder, Colo., 1987.

Wolff, G.T., and R.L. Klimisch, (Eds.), *Particulate Carbon: Atmospheric Life Cycle*, 411 pp., Plenum, New York, 1982.

Wolff, G.T., R.J. Countess, P.J. Groblickie, M.A. Ferman, S. Cadle, and J.L. Muhlbaier, Visibility-reducing species in the Denver "Brown Cloud", II, Sources and Temporal Patterns, *Atmos. Environ.*, *15*, 2485–2502, 1981.

Wolff, G. T., M.S. Ruthkosky, D.P. Stroup, P.E. Korsog, M.A. Ferman, G.J. Wendel, and D.H. Stedman, Measurements of SOx, NOx, and aerosol species on Bermuda, *Atmos. Environ.*, *20*, 1229–1239, 1986.

Yaaqub, R.R., T.D. Davies, T.D. Jickells and J.M. Miller, Trace elements in daily collected aerosols at a site in southeast England, *Atmos. Environ.*, *25*, 985–996, 1991.

Zhang, S.H., M. Shaw, J.H. Seinfeld, and R.C. Flagan, Photochemical aerosol formation from α-pinene and β-pinene, *J. Geophys. Res.*, *97*, 20,717–20,729, 1992.

Zimmermann, P.H., J. Feichter, H.K. Rath, P.J. Crutzen, and W. Weiss, A global three-dimensional source-receptor model investigation using 85Kr, *Atmos. Environ.*, *23*, 25–35, 1989.

H. Cachier and C. Liousse, Centre des Faibles Radioactivités, Laboratoire Mixte CNRS-CEA, Ave de la Terrasse, 91198 Gif sur Yvette, France.

C. Chuang, H. Eddleman, and J.J. Walton, Atmospheric Science Division, Lawrence Livermore National Laboratory, L-240, Livermore, CA 94551.

J.E. Penner, Lawrence Livermore National Laboratory, 7000 East Avenue, L-240. Livermore, CA 94550. (e-mail: joyce.penner@quickmail.llnl.gov)

(Received January 31, 1995; revised September 7, 1995; accepted October 13, 1995.)